ISTANBUL TECHNICAL UNIVERSITY ★ GRADUATE SCHOOL OF SCIENCE ENGINEERING AND TECHNOLOGY

PREPARATION AND CHARACTERIZATION OF FUNCTIONALIZED SEPIOLITIC CLAY NANOFIBERS : ANTIBACTERIAL ACTIVITY AND CONDUCTIVE-AFM STUDY

M.Sc. THESIS

Nihan Cansu YALIN

Department of Nanoscience & Nanoengineering

Nanoscience & Nanoengineering Programme

JANUARY 2014

ISTANBUL TECHNICAL UNIVERSITY ★ GRADUATE SCHOOL OF SCIENCE ENGINEERING AND TECHNOLOGY

PREPARATION AND CHARACTERIZATION OF FUNCTIONALIZED SEPIOLITIC CLAY NANOFIBERS : ANTIBACTERIAL ACTIVITY AND CONDUCTIVE-AFM STUDY

M.Sc. THESIS

Nihan Cansu YALIN
(513101013)

Department of Nanoscience & Nanoengineering

Nanoscience & Nanoengineering Programme

Thesis Advisor: Assoc. Prof. Dr. Birgül BENLİ

JANUARY 2014

İSTANBUL TEKNİK ÜNİVERSİTESİ ★ FEN BİLİMLERİ ENSTİTÜSÜ

SEPİYOLİT NANOFİBERLERİNİN FONKSİYONELLEŞTİRİLMESİ VE KARAKTERİZASYONU: ANTİBAKTERİYEL AKTİVİTE VE AFM-İLETKENLİK ÖLÇÜMLERİ

YÜKSEK LİSANS TEZİ

Nihan Cansu YALIN
(513101013)

Nanobilim & Nanomühendislik Anabilim Dalı

Nanobilim & Nanomühendislik Programı

Tez Danışmanı: Doç. Dr. Birgül BENLİ

OCAK 2014

Nihan Cansu YALIN, a **M.Sc.** student of ITU **Graduate School of Science, Engineering and Technology** student ID **513101013**, successfully defended the **thesis** entitled "**PREPARATION AND CHARACTERIZATION OF FUNCTIONALIZED SEPIOLITIC CLAY NANOFIBERS: ANTIBACTERIAL ACTIVITY AND CONDUCTIVE-AFM STUDY**", which she prepared after fulfilling the requirements specified in the associated legislations, before the jury whose signatures are below.

Thesis Advisor :	**Assoc. Prof. Dr. Birgül BENLİ** İstanbul Technical University	....
Jury Members :	**Assoc. Prof. Dr. Hüseyin KIZIL** İstanbul Technical University	....
	Assoc. Prof. Dr. Sevil YÜCEL Yıldız Technical University	....

Date of Submission : December 2013
Date of Defense : January 2014

To my grandmother,

FOREWORD

In the process of writing my thesis, I have received a great amount of support from many people. First, I would like to thank my thesis advisor Assoc. Prof. Birgül BENLİ, who has been guiding and encouraging me with patience. Without her advice and support, I would not have been able to complete my MSc. thesis.

Besides, I am grateful to my friends and colleagues for their kind concern and great encouragement to me. They were always willing to give their helping hands when I was in need.

Last, but definitely not least, I would like to thank my family for their endless love and support, for their unwavering confidence in me, and for their limitless patience. I managed to come to a long journey this far with their support.

I dedicate this thesis to my grandmother who passed away right before I hand out my thesis, I will always feel her presence with me.

December 2013

Nihan Cansu YALIN
(Biology Graduate)

TABLE OF CONTENTS

Page

ABBREVIATIONS

AAS	**:** Atomic Absorption Spectrometry
AFM	**:** Atomic Force Microscopy
E.coli	**:** *Escherichia coli*
EFM	**:** Electric Force Microscopy
FTIR	**:** Fourier transform infrared spectroscopy
I-AFM	**:** Current-Atomic Force Microscope
KAO	**:** Kaolen
LB	**:** Luria-Bertani
MIC	**:** Minimum inhibitory concentration
MMT	**:** Montmorillonite
NM	**:** Nanometre
PAL	**:** Palygorskite
PPM	**:** Parts per million
SAM	**:** Ampicillin/sulbactam
S.aureus	**:** *Staphylococcus aureus*

LIST OF TABLES

Page

LIST OF FIGURES

Page

PREPARATION AND CHARACTERIZATION OF FUNCTIONALIZED SEPIOLITIC CLAY NANOFIBERS : ANTIBACTERIAL ACTIVITY AND CONDUCTIVE-AFM STUDY

SUMMARY

Nanofibers are the materials in fiber form that have diameter equal to or less than 100nm. Nowadays, its potential applications include filtration devices, textile industry, tissue engineering scaffolds, sensors, membrane and coating materials development, electronic applications, etc. The need of high-quality nanofiber is increasing every day depending on the developments in high-tech materials. Natural clay is one of the alternative biodegradable fiber materials for the use of these innovative applications. In natural fiber clays, sepiolite fibrous has an special importance due to the fact that Turkey has the second biggest sepiolite reserve on the earth. Sepiolite belongs to a group of layered silicates with a magnesium hydrosilicate chemical formula. It is used as fillers in numerous applications due to its fibrous structure, high surface area, porosity, crystal morphology and composition, surface activity, production of stable dispersions at low concentrations. These properties provide a basis for varieties of catalytical, sorptive and rheological application such as pet litter, detergents, drugs and ceramics. However, nanotechnological applications such as nanocomposites, antibacterial nanocoatings, sensors and bio-MEMS need high-quality sepiolite nanofibers. Sepiolite deposits are possessed of major impurities such as dolomite, calcite, and others, magnesite paligorskit, quartz, feldspar, and phosphates. Due to very fine particle sizes (<2 μm), the removal of impurities is still a problem without breaking the fibers of sepiolite.

High-quality sepiolite nanofibers deliberated by high-speed mixers and separated from impurities using gravity separation techniques. After obtained the sepiolite fibrous, Ag^+ and Cu^{2+} loaded sepiolites were prepared. According to adsorption isotherms, antibacterial activity of Ag^+ and Cu^{2+} loaded sepiolite fibers was tested for *E.coli* and *S.aureus* by two common methods: serial dilution and disk diffusion method. Results showed that minimum inhibitory concentrations of each solutions were determined as 50mg/L Ag^+ and 100mg/L Cu^{2+} - loaded sepiolite samples, respectively. Besides, this study proved that silver is a stronger antibacterial agent than copper since gram-negative bacteria *E.coli* is more resistant to antibacterial clay agents than *S.aureus*. After washing the treated clay samples with distilled water five times, the samples maintained their antibacterial activity and were just as effective as the first time in the second trials.

AFM and EFM/I-AFM measurements will be performed to indicate topography and the electrical conductivity of the sepiolite samples. Scanning the surface of sepiolite thin films by the combined AFM/current technique can lead to requirements in local functionalization of their electronic properties. This change in local properties is made and correlated with copper and silver adsorption studies.

According to change of current amplifier, External I-AFM mode referred to the I-AFM that uses the external low noise current amplifier named as Ultra-Low Noise Conductive AFM (ULCA), silver loaded sepiolite films showed promising results compared to the copper functionalized sepiolite films while raw sepiolite has no electrical conductivity. To decrease the effect of morphology of these clay films, each measurement was focused and applied on a single sepiolite nanofiber. As expected, these results are in agreement with an electrostatic force microscopy (EFM) study, showing that the electrons were transferred rapidly to the surface of Ag-Sepiolite film, compared with that on either pure sepiolite clay film or Cu-sepiolite film. This is a great potential for improving cheaper, durable, biodegradable innovative applications in clay thin films.

Sepiolite fibers separated from its impurities and loaded with silver and copper ions show excellent antibacterial activity as well as good electrical conductivity. These modified high-quality sepiolite nanofibers have big potential for nanotechnological and biomedical applications.

SEPİYOLİT NANOFİBERLERİNİN FONKSİYONELLEŞTİRİLMESİ VE KARAKTERİZASYONU: ANTİBAKTERİYEL AKTİVİTE VE AFM-İLETKENLİK ÖLÇÜMLERİ

ÖZET

Nanofiberler, 100nm ya da daha küçük çaptaki fiber formlarıdır. Günümüzde nanofiberlerin potansiyel kullanım alanları tekstil endüstrisi, filtrasyon cihazları, doku mühendisliği iskelet yapısı, sensör ve membran çalışmaları, yüzey kaplama maddelerinin geliştirilmesi ve elektronik uygulamalardır. Yüksek teknolojiye sahip ürünlerin geliştirilmesinde yüksek kaliteli nanofiberlerin kullanım ihtiyacı gün geçtikçe artmaktadır. Geri dönüştürülebilir fiberlere sahip doğal killer bu amaçla kullanılmak üzere en uygun adaylardandır. Sepiyolit, magnezyum silikat yapılı olup, en bilinen tabaka yapılı kil olan montmorillonitten farklı olarak, emsalsiz fiberlere sahiptir. Yapısındaki bu eşsiz kanal ve tüneller sepiyolite üstün adsorpsiyon ve yüzey özellikleri sağlamaktadır. Bu sayede sepiyolit, yüksek dayanımlı, nemden etkilenmeyen, daha ucuz ve tamamiyle doğal bir malzeme olmasından dolayı MEMS, sensör gibi çalışmalarda kullanılmak için idealdir.

Öte yandan, killer üzerine yapılan çalışmaların büyük bir çoğunluğunda tabakalı yapıda bulunan montmorillonit tipi smektit grubu killerle yapılmış olup, fiber yapılı sepiyolitler ile ilgili çok az sayıda çalışma mevcuttur. Sepiyolit üzerine yapılan bilimsel araştırmalar ve çalışmaların büyük bir kısmı sepiyolitin adsorpsiyon ve reolojik özellikleriyle ilgili çalışmalardır. Hatta sepiyolitten nanokompozit eldesi ile ilgili yayın sayısı oldukça sınırlıdır. Ülkemizin dünyanın ikinci büyük sepiyolit rezervlerine sahip olmasından dolayı üretilecek sepiyolit/sepiyolit katkılı malzemelerin Türk sepiyolitleri adına ne denli öneme sahip olduğu açıktır.

Bu tezde öncelikle sepiyolit liflerinden dolomit, albit, quartz, kalsit, montmorillonit vb. safsızlıkların uzaklaştırılması için gravite yöntemi esaslı eşiksiz sallantılı masa olan Mozley masası ile çalışılmıştır. Safsızlıkları uzaklaştırılmış sepiyolit daha sonra, literatürde de sıkça bahsedilen yüksek hızlı karıştırma işlemine tabi tutularak, fiberlerin düzgün bir şekilde dağıtıldığı bir sistem geliştirilmiştir. Lakin bu süre aşıldığında sepiyolit liflerinin kırılarak parçalanmakta olduğu tespit edilmiştir. Mekanik karıştırma ile birlikte Mozley masasında zenginleştirme çalışmalarının faydalı olduğu görülmüştür.

Fiberlerin hem elektriksel özellikleri ve hem de antibakteriyel aktivitelerinin geliştirilmesi için gümüş ve bakır adsorpsiyonu çalışmaları yapılarak, Ag^{+} ve Cu^{2+} ilaveli sepiyolit fiberleri geliştirilmiştir. Bu çalışmalar için farklı konsantrasyonlarda gümüş nitrat ve bakır sülfat çözeltileri hazırlanmış, sepiyolit örnekleri ile farklı konsantrasyonlarda gümüş nitrat ve bakır sülfat çözeltileri belli süre muamele edilmiştir. Sürenin sonunda santrifüj edilen killer filtrasyon ve kuruma işlemlerinden sonra geri kazanılmış, santrifüj sonrası supernatant kısımdan alınan örneklerin gümüş ve bakır içeriği atomik absorpsiyon spektroskopisi ile ölçülmüştür. Elde edilen değerlere göre yapılan hesaplamalar sonucu adsorpsiyon izotermleri ortaya konulmuş, kile maksimum yüklenebilecek iyon miktarı belirlenmiş ve sepiyolit yüzeyine bu iyonların fiziksel adsorpsiyonla bağlandığı gösterilmiştir. Langmuir adsorpsiyon modeli her iki iyon için de en uygun model olarak bulunmuştur.

Antibakteriyel aktivite çalışmaları için saf, Ag^{+}, Cu^{2+} ilaveli sepiyolit örnekleri gram negatif bir bakteri olan *E.coli* ve gram pozitif bir bakteri olan *S. aureus* türüne karşı denenmiştir. Bu deneyler için seri dilüsyon ve disk difüzyon yöntemi kullanılmıştır. Seri dilüsyon yöntemi ile gözle görülen mikrooganizma üremesini engelleyen en düşük değer olan minimum inhibisyon konsantrasyonu belirlenmiştir. Bu değer Ag^{+} yüklü killerde 50mg/L olarak bulunurken, Cu^{2+} ilaveli sepiyolit örneklerinde ise 100mg/L olarak tesbit edilmiştir. Deney sonuçlarına göre, gümüşün bakıra göre daha iyi bir antibakteriyel ajan olduğu ve gram pozitif bakterilerin negatif yüklü dış membranlarının gram negatif bakterilere göre daha kalın olmasından dolayı elektrostatik etkileşimler sonucu pozitif yüklü iyonlarla daha fazla temas halinde oldukları, bu nedenle de bu iyonlara karşı daha savunmasız oldukları ortaya konulmuştur. Bu bulgular literatürdeki çalışmalar ile de desteklenmiş ve mekanizmalar açıklanmıştır. İyon değişimi gerçekleştirilmiş örnekler distile su ile 5 kez yıkandıktan sonra bile ilk seferdeki antibakteriyel etkiyi gösterdiği de daha sonraki deneylerle ortaya konulmuştur.

Çalışmanın AFM (Atomic Force Microscopy) takipli görüntü analizlerinden sepiyolit fiberlerinin boyutu tesbit edilmiştir. AFM görüntüleri sepiyolit fiberlerinin iki boyutunun nano ölçekte olduğunu ortaya koymuştur. Bu çalışmalara ek olarak, yüzeylerin yarı iletkenlik özellikleri Conductive-AFM ve EFM (Electrostatic Foce Microscopy) ile ölçülmüştür. İletkenlik sonuçlarına göre saf sepiyolit fiberleri ölçüm aralıklarında elektriği tek başına iletemezken, Ag^{+} ve Cu^{2+} katkısı ile yarı iletken sepiyolit nanofiberi üretimi mümkün olmaktadır. Özellikle Ag^{+} iyonu Cu^{2+} iyonuna göre sepiyolit fiberlerine daha iletken özellik katmaktadır. Buradan hareketle, gümüş ve bakır ilaveli sepiyolit fiberlerinin hem iyi birer antibakteriyel ajan oldukları ve hem de elektriği iletebildikleri tespit edilmiştir.

Tüm bu deneyler sonucu, safsızlıklarından uzaklaştırıp, Ag^{+} ve Cu^{2+} iyonu yükleyerek geliştirmiş olduğumuz hem iyi bir antibakteriyel ajan ve hem de iyi bir yarı iletken olan sepiyolit fiberlerinin sensör, antibakteriyel yüzey kaplaması, nanokompozit, biyoMEMS, güneş pilleri gibi ileri nanoteknolojik ve biyomedikal uygulamalarda kullanılmak için potansiyel taşıdığı ve çalışmalarımızın bu yönde devam ettiği yorumu yapılmıştır.

1. INTRODUCTION

1.1 Purpose of Thesis

The purpose of this thesis is to functionalize the sepiolite clay nanofibers in the characterstics of good antibacterial activity and electrical semi-conductivity, also use for further nanotechnological applications as a novel nanomaterial. In this regard, the product of high-quality sepiolite nanofibers were separated from impurities by using mozley table gravity separation method which is a simple way for quick and efficient separation of mineral grains of a certain size class, followed by other selected size fractions. Produced sepiolites were carried out for Ag^{+} and Cu^{2+} adsorption experiments. In these experiments, Ag^{+} and Cu^{2+} exchanged sepiolite samples were prepared and their adsorption isotherms analyzed. Also best adsorption model was chosen. Since the antibacterial properties of silver and copper have been known for a very long time, these two ions were used as antibacterial agents. Antibacterial activity of Ag^{+} and Cu^{2+} exchanged sepiolite samples were tested against two different bacteria strains *E.coli* and *S. aureus* by serial dilution and disk diffusion method. Finally, AFM and EFM/I-AFM measurements were performed to indicate topography, nanofiber size and then the electrical conductivity of the raw, Ag^{+} and Cu^{2+} exchanged sepiolite samples.

2. LITERATURE REVIEW

2.1. Nanofibers and Their Applications

Nanofibers are a nanomaterial, with diameters less than 100nm. However, textile industry accepts fiber diameters below 1000nm. Nanofibers can be used in many different applications because of their, enormous specific surface area, small pore size, good breathability, high porosity and possibility to incorporate different additives (Petrik, 2011). As the fiber length or diameter increases, the average strength of the fiber decreases. This behavior is shown by organic fibers such as cotton, aramid, as well as inorganic fibers such as tungsten, silicon carbide, glass or alumina (Elices and Llorca, 2002). Most common nanofibers are polymeric, carbon, metallic, glass and ceramic nanofibers.

Polymeric nanofibers widely used in various important applications. For the fabrication of polymeric nanofibers, electrospinning has been regarded as the most promising approach to produce continuous nanofibers on a large scale and the fiber diameter can be adjusted from nanometers to micrometers (Li and Xia, 2004). Various polymers have been successfully electrospun into ultrafine fibers in solvent solution and some in melt form.

Inorganic nanofibers are composed of ceramic, metal oxides or fibrous clays and produced in bulk and require additional processing or calcinations to remove organic compounds from the material. The main applications for inorganic nanofiber usage are catalysis (e.g. photocatalysis), electrode materials, sensors, nanocomposites (increasing of mechanical properties, electric and magnetic properties etc.), in medicine and cosmetics.

Several methods have been developed to fabricate nanofibers, such as template (Ikegame et al., 2003), self-assembly (Hong et al., 2003), phase separation (Ma and Zhang, 1999), meltblowing (Ellison et al., 2007) and electrospinning (Doshi and Reneker, 1995; Lin et al., 2004; Lin et al., 2005; Fang et al., 2007; Xue et al., 2009;

Fang et al., 2010). The modification and functionalization of nanofibers using various chemical or physical processes can significantly improve surface properties, for example creating super-hydrophobic (water repellent) or super-hydrophilic (highly water absorbent) materials.

Further development of nanofibers carrying hope for finding solutions to fundamental problems of human society, such as cleaning and production of drinking water, batteries enabling advanced energy storage. Thus, nanofibers have huge demand and the potential of nanofibers represents good opportunities for business. Outstanding properties of nanofibers make them suitable candidate for a wide range of applications from medical to textile products and industrial to high-tech applications for aerospace, capacitors, transistors, drug delivery systems, filtration, barriers, wipes, sensors, composites, garments, insulation, battery separators, energy storage and fuel cells (Lee and Bhat, 2003).

Industrial	**Healthcare**	**Energy**	**Retail**
Filtration	Wound care	Battery membranes	Nonwovens
Barriers	Tissue scaffolds	Solar Cells	Hygiene
Nanocomposites	Barriers		Lightweight
Sensors	Sensors		Lighting
Acoustic insulation	Drug Delivery		Thermal
Anti-microbial	Anti-microbial		

Figure 2.1 : Nanofiber Application Areas (Petrik, 2011).

2.1.1. Fibrous clays

Many of the clay minerals have a fibrous habit under some conditions. Non-lamellar structural arrangement such as tubular halloysite and imogolite, but more frequently sepiolite and palygorskite fibrous clays, have become attractive as alternative fibrous clays. Three-dimensional ordering of phyllosilicates creates open channels containing both zeolitic and crystallization water. The presence of zeolitic channels and the fibrous crystalline structure are the main reasons why sepiolite and palygorskite have such notable rheological, adsorbent and catalytic properties (Galindo, 2011).

The crystalline structure of both sepiolite and palygorskite microfibrous clays is related to talc-like ribbons parallel to the fiber axis that can be regarded as structural blocks alternating with structural cavities, named tunnels, associated with the internal surface of the silicates that grow up in the fiber direction (Fig. 2.2). The tunnels acceding to the external surfaces of fibrous clays are termed as channels.

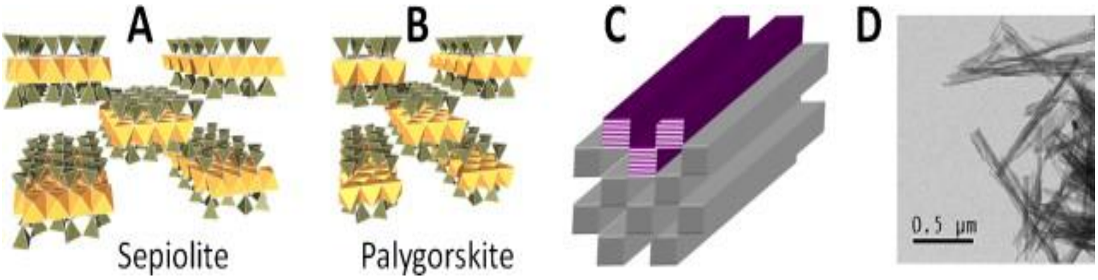

Figure 2.2 : Schematic representation of structural and textural features of fibrous clay minerals: A) sepiolite structure; B) palygorskite structure; C) ideal representation of the cross-section of sepiolite fiber based on (Ruiz-Hitzky, 2001). D) TEM image of sepiolite (Pangel S9, from TOLSA, Madrid, Spain).

Like all phyllosilicate minerals containing 2:1 layers where there is an octahedral sheet between two opposing tetrahedral sheets, sepiolite has continuous planes of tetrahedral basal oxygen atoms. But, unlike other 2:1 phyllosilicates, the apical oxygen atoms point away from the basal oxygen atom plane in opposing directions to form ribbons of joined pyroxene-like chains (Guggenheim, 2010). The discontinuity of the tetrahedral sheets gives rise to the presence of silanol groups (Si–OH) at the edges of the tunnels, which are the channels opened to the external surface of the sepiolite particles (Huang et al., 2010).

2.1.2. Properties of sepiolite and its applications

Sepiolite, structurally similar to palygorskite, intersilite, amphibole, and raite, is one of the most important industrial magnesium-rich in 2:1 phyllosilicate clay minerals, i.e. octahedral layer is bound above and below by a silica tetrahedral sheet (Kogel et al., 2006). Since the discontinuous octahedral sheets extend only in one dimension, the tetrahedral sheets are divided into ribbons by a periodic inversion of rows of tetrahedrons. The very large channels or tunnels are located between these ribbon strips and formed chainlayer molecular structure of sepiolite mineral as well as its unique fibrous structure (Figure 2.3). Chain-layer molecular structure exactly determines the hydrophobicity and anisotropic character of sepiolite within the half-cell formula of $Mg_4Si_6O_{15}(OH)_2.6H_2O$. While hydrogen bonding sides of silanol groups (Si-OH) are presented on the external surface; owing to discontinuities and chain-layer molecular structure, Mg^{2+} ions located at the edges of octahedral sheets exert more influence on the hydrophobicity of sepiolite (Ruiz-Hitzky, 2001; Benli et al., 2012). In other words; the breakage of Si-O and Mg-O bonds provides many hydrogen bonding sites on the sepiolite edge surfaces similar to the natural hydrophobic talc mineral whose edge surfaces facilitate the formation of strong hydrogen bonds with water dipoles (Du et al., 2007).

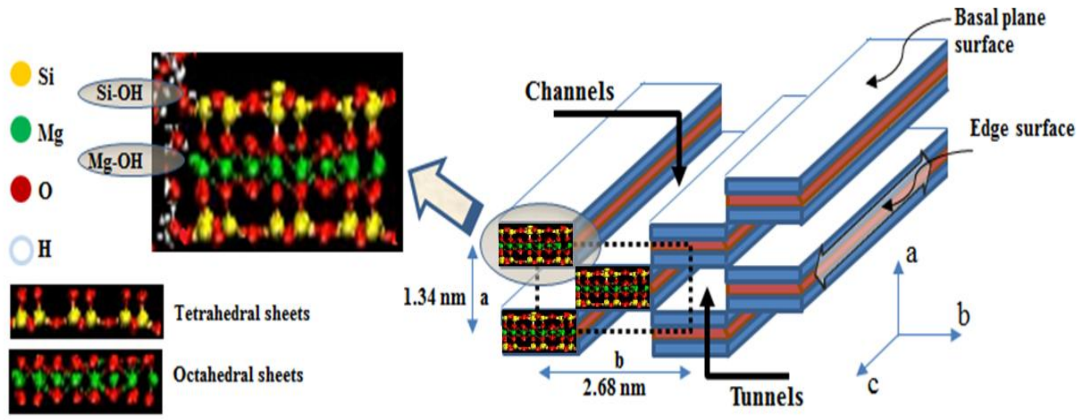

Figure 2.3 : MD simulation snopshot of equilibrated water/sepiolite surface. The color representations are: red – oxygen atoms, white-hydrogen atoms, yellow – silicon atoms and green – magnesium atoms. 2:1 layers, an octahedral sheet between two opposing tetrahedral sheets; discontinuous octahedral sheets extend only in one dimension, the tetrahedral sheets are divided into ribbons. Channels or tunnels located between these ribbon strips (Benli et al. 2012).

The structure and chemical properties of sepiolite is almost identical to palygorskite; except it has a slightly larger unit cell and some of the magnesium cations have been replaced by aluminium or iron. Composition and morphology of these fibrous clays can fluctuate very much from one deposit to another. Sepiolite shows typical fiber length of about 1–2μm, although in certain cases (e.g. China, Finland) the fibers are much longer. Typical dimensions of the cross-section of a sepiolite fiber from Vallecas (Spain) are 25 × 4 nm, which corresponds to about nine unit cells in width and only three in thickness. The AFM study revealed that the average fiber dimensions at the highest viscosity were determined as 249 × 1127 × 29 nm (width × length × height) (Can et al., 2010).

In contrast to bentonitic clays, fibrous clays have non-swelling properties and their structure is more stable; they can be used as bundles or individual needles. However, these fibrous clays have a tendency to agglomerate. In this regard, according to the required applications nanofiber dispersion methods may be used to prevent their agglomerations. As shown in Fig. 2.4, if the bundles of fibers are dispersed in water with a mechanical stirrer, these fibers randomly form networks which increase the suspension viscosity (Santaren, 1993, Bokobza, 2004 and Bokobza et al., 2004). At constant solids concentration, most of these fibers will be dispersed and the viscosity will increase depending on the ability of inner and outer surfaces of particles interacting with water molecules and each other. Meanwhile, the network structure is formed with the hydrogen bonds between silanol groups under surface forces like van der Walls attractive forces (Santaren, 1993 and Çınar, 2005).

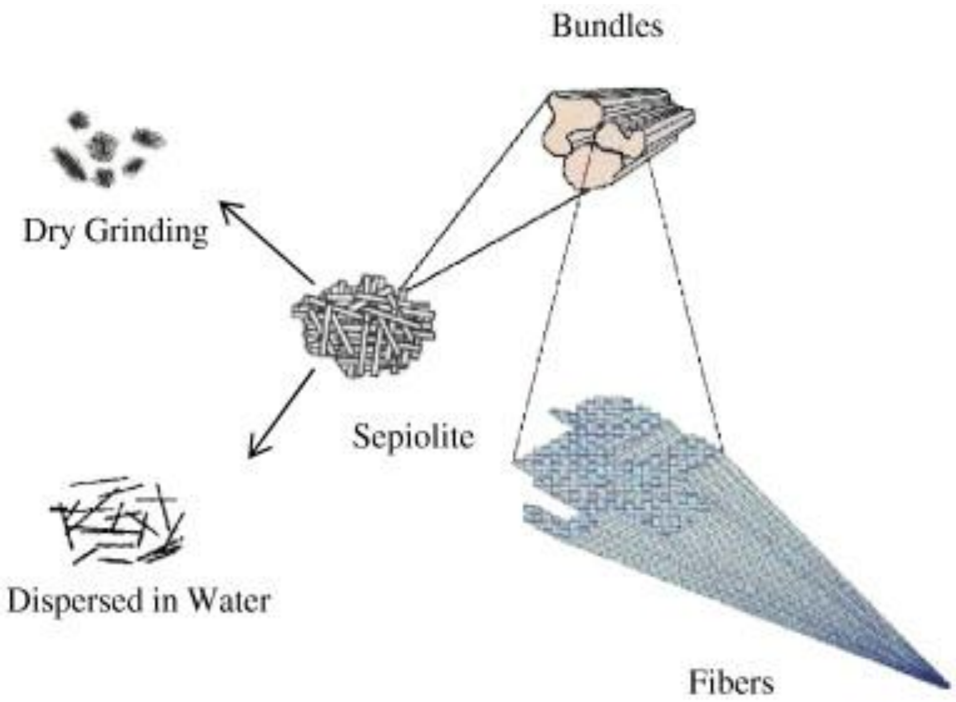

Figure 2.4 : Schematic representation the aggregation of sepiolite fibers (Grupa Tolsa Madrid, Spain).

The properties of sepiolite and palygorskite can be changed by various types of treatments applied to the raw material. As a result of these procedures six different generations are indicated for applications so far.

Table 2.1 : Six generation of products and applications of sepiolite (Alvarez et al., 2011).

GENERATION PRODUCT	INDUSTRIAL TREATMENTS	APPLICATIONS	EXAMPLES
First	Conventional crushing, grinding and sieving	Absorbent products, carriers	Pet litter, bedding for poultry, absorbents for greases, oil, water and other chemicals, floor and industrial absorbent, carriers of agricultural chemicals and catalysts, animal feeds, moisture control and filtration of fuels and oils.
Second	Micronization processes	Fillers and rheological additives for water-based system	Rheological additives in paints and coatings, bitumen anionic emulsions, modified asphalt, liquid animal feeds, mortars, dry and wet shotcrete, fluid fertilizers and processing aids.
Third	Organic surface treatment	Rheological additives for solvent-based system	Solvent-based paints, primers, greases, solvent asphalt coatings, inks, adhesives, foundry washes, epoxy systems and plastisols.
Fourth	Synergistic combinations with additives	Enhanced adsorbents and rheology modifiers	CIMSIL (modified sepiolite additives manufactured by Tolsa), PANGEL (organically modified sepiolite commercial product by Tolsa).
Fifth	Chemical modification of the structure to enhance physico-chemical characteristics	Fibrous silicas and high CEC sepiolites	Special fillers and carriers for catalysts obtained from fibrous silica derived from sepiolite, additives for Fluid Catalytic Cracking (FCC) processes such as aluminium-exchanged synthetic loughlinite (a variety of sepiolite)
Sixth	Sepiolite-based nanomaterials	Sepiolite nanoclays and functional sepiolites	Nanoadditives for polymers and sepiolite functionalized with nanoparticles

The large surface area and the resistance to chemical reactions make the sepiolite perfect carrier for scents, oxidizing agents, catalysers, and used for filtration to purify organic liquids. This clay has a high absorption capacity and a high degree of interaction with polymers. Sepiolite is also used as a rheological additive for mortar, plaster and concrete to improve their properties in both the fresh and the hardened state. Its rheological behaviour is stable in a broad pH range, at high electrolyte concentrations and temperatures. Sepiolite acts as a thixotropic and an anti-sagging/anti-slipping agent improving workability, adherence to the substrate, pumpability and surface finish. With the shear effect accompanying micronization, dispersion of the clay particles is achieved, thus sepiolite additives can be used in the solidification and immobilization of toxic waste liquids or sludges (Alvarez et al., 2011).

As for health and safety issues, sepiolite is generally considered as safe, and it is authorized by the EU as animal feed additive. Besides, a wide investigation is carried out from epidemiological to different studies including inhalation, intrapleural and intraperitoneal inoculation. No result has shown inhalation of sepiolite dust can cause lung diseases and no incidence of tumours has been observed in animal studies (Santaren and Alvarez, 1994). Also studies on humans exposed to sepiolite dust have shown that there is no risk of pulmonary disease, with no evidence of pleural plaques or mesothelioma (Governa et al., 1995; McConnochie et al., 1993). Moreover, contact with these minerals does not represent any risk at all.

2.1.3. Nanofiber dispersion techniques

The process of deagglomeration and distribution of nanofibers within matrices or solvents is called dispersion. Nanofibers have strong tendency to agglomerate because of the attractive forces such as Van der Waals and etc. Therefore, stronger forces than inter-particle adhesion forces are needed. Dispersion can occur either splitting up the agglomerates into small fragments under high stress (rupture) or due to continuous detachment of small fragments at a comparatively lower stress (erosion) (Parveen, 2013). Mostly water is used as a carrier to disperse nanofibers, also other chemical and physical treatments are used to overcome agglomeration and entanglement.

Chemical Modification methods: Different chemical methods have been used to achieve homogeneous dispersion of nanofibers in water (Zhu et al., 2004) and various polymers such as using organic solvents (Ausman et al., 2000) surfactants (Holbery and Houston, 2006; Paredes et al., 2004) such as sodium dodecyl sulphate, SDS, and sodium dodecyl benzenosulfonate, SDBS (Bystrzejewski et al., 2010), coupling agents such as stearic acid, mineral oil and maleated ethylene (Saheb and Jog 1999) functionalization with acids such as Carboxylic Acid (Peng et al., 2003), amines (Wang et al., 2005), fluorines (Lavskaya et al., 2009), and matrix moieties (Gonzalez et al., 2012), noncovalent functionalization with oligothiophene-terminated poly-ethylene glycol (Lee et al., 2007), using block polymers (Xin et al., 2008; Nativ-Roth et al., 2007), wrapping conjugated polymers such as Polyacrylonitrile (Seneewong et al., 2013) and hydroxylamine hydrochloric acid salt (Sabba et al., 2004).

Physical Modification methods: Physical treatments can change structural and surface properties of the fiber, physical methods involve surface fibrillation, electric discharge, ultrasonication, irridation, UV Radiation/Gamma Radiation/Electron Radiation (Evora et al., 2013) and electric currents (Belgacem et al., 1994; 1995) Surface modification by discharge treatment such as low temperature plasma (Vande Wielen and Ragauskas, 2006), plasma, microwave sputtering and corono discharge have been used (Bataille et al., 1989; Dong et al., 1993; Yuan et al., 2002) Ultrasonication is commonly used as a disruptive force in laboratory scale dispersion (Higashitan et al., 1993; Ping et al., 2008 and Samir et al., 2004) Industrial scale dispersion, media milling is another common technique when micron size beads are used as grinding media, the dispersion of nano-order particles (Inkyo et al., 2006 and Gotoh et al., 2009)

Defibering treatment of sepiolite as a simple and cheap way to obtain mineral nanofibers, also by using surface modification agents such as octyltrimethoxysilane (Volle et al., 2012), hexadecyltrimethylammonium bromide (Tunc et al., 2011) and cuprous oxide (Zhu et al., 2012).

2.2. Properties and Applications of Clay-Nanocoatings

Nano-coatings are usually applied as multi-layered systems that are composed of primer and topcoat. Each coating layer is applied to perform specific functions, though its activities are influenced by the other layers in the system. The interactions among different layers and the interfacial phenomenon play an important role in the overall performance of the multi-coat systems (Hegedus, 2004). Most coatings (whether inorganic, organic or ceramic) perform critical functions, such as durability, reproducibility, easy application and cost effectiveness, tailored surface morphology, environmental friendliness. Addition of nano-material or nano fillers to the coatings improves the properties of the conventional coatings and produces new multi-functional coating due to their tiny particle size (Mathiazhagan and Joseph, 2011).

Anti-corrosive coatings: Layered clay montmorillonite is introduced into organic resin systems to increase the barrier effect towards oxygen and water molecules to enhance the anticorrosive performance of the coating (Yeh et al., 2004). Recent developments also include the use of nanoclay that can exchange anticorrosive agents with the corrosive species when needed (Mathiazhagan and Joseph, 2011). Advanced anticorrosive coatings can be prepared from polymer-clay nanocomposite materials (Bagherzadeh et al., 2011), studies on preparation of epoxyclay nanocomposite coating by shown that incorporating nanoclay particles into organic coatings improves anti-corrosive properties of coating.

High thermal-resistant, fire-retardand coatings: Polymer clay nanocomposites have also been used for high thermal-resistant, fire-retardand coatings (Chen et al., 2012). The synergistic effects of organo-sepiolite (OSEP) and zinc borate (BZn) on the fire retardancy of polypropylene (PP) were studied (He et al., 2013). The influence of the incorporation of polyamide-6 (PA) and natural sepiolite nanoparticles on both the thermal degradation and fire behaviour of PP matrix has also been investigated (Laoutid et al., 2013) The peak heat release rate of PP/sepiolite and PP/organo-sepiolite composites, with 10% sepiolite loading, decreased by 54% and 66%, respectively (Caoa et al., 2012). Sepiolite has excellent absorbability and fine thermal capacity, and the elements like magnesium and silicon are possess are themselves excellent halogen-free flame-retardant, and are nontoxic, harmless and abundantly available, presenting great potential in flame retarding and smoke suppression. The synergy between sepiolite and magnesium hydroxide (MH) in halogen-free flame retardant ethylene-vinyl acetate (EVA) copolymer was investigated, the cone calorimeter test (CCT) data indicated not only the reduction of heat release rate (HRR) and mass loss rates (MLR), but also prolonged ignition time (TTI) and depressed smoke release (SR) were observed during combustion (Huang et al., 2010) Sepiolite nanofibers can also used for thermal insulation coatings (Chen et al., 2010).

Self cleaning coatings: These type of coatings clean themselves through the action of water, the former by rolling droplets and the latter by sheeting water that carries away dirt. Due to absence of hydrogen bonding sites, the sepiolite basal plane is considered as hydrophobic (Benli et al, 2012). On the other hand sepiolite is modified with different agents to get hydrophobic property (Le et al., 2012) Thus sepiolite is a promising material to be used with polymers to form hydrophobic nanocomposite coatings. Fluorosilica/sepiolite hybrid composite materials showed good antistaining properties in the writing and erasing test on a glass substrate up to eight times (Sunga et al., 2013), sepiolite used as a support for enzyme immobilization of urease, this behaviour has been related to the existence of protein-clay hydrophobic interactions (Segura et al., 1987).

Antifouling coatings: Both biocidal and nonbiocidal coatings are used to prevent foulings. Biocide based antifouling coatings function by slow leaching of the incorporated biocides into the coating. Usage of biocides is restricted on daily basis because of the legislations and toxicity. As an alternative, sepiolite mineral can be used instead of biocides, because it has no toxic effect and it is all natural also can show slow leaching of antibacterial agent. Silver and copper functionalized sepiolite-polylactic acid membranes anti-biofouling efficiency was measured, silver-sepiolite yielded a 35% biofouling decrease in contact with *P. putida* and a remarkable 85% for *S. cerevisiae* (Rosal, 2012). Fouling-release coatings are made from poly(dimethyl siloxane) PDMS elastomers. To improve the mechanical properties of PDMS, polymer is reinforced by adding carbon nanotubes and/or natural sepiolite fillers (Beigbeder et al., 2008).

Nanopolymer coatings: Conducting polymers have evoked a great deal of interest due to their electrochemical properties and their mixed ionic/electronic conductivity properties (Rout et al., 2003). A conducting polymer modified with sepiolite was utilized in the construction of a highly sensitive and fast amperometric cholesterol biosensor, by this way a novel accurate and inexpensive cholesterol biosensor was developed for the determination of total cholesterol in food samples (Soylemez et al., 2013). Sepiolite-graphenelike carbon nanocomposite presents higher electronic conductivity than it is disordered graphenelike carbon component (Alvarez et al., 2012).

2.3. Properties and Applications of Antibacterial Agents

Antibacterial agents can be anything that destroys bacteria or suppresses their growth or their ability to reproduce. Unlike antibiotics, they are not used as medicines for humans or animals, but are found in products such as soaps, detergents, health and skincare products and household cleaners.

Antibacterials may be divided into two groups according to their speed of action and residue production: The first group contains those that act rapidly to destroy bacteria, but quickly disappear (by evaporation or breakdown) and leave no active residue behind, such as alcohols, chlorine, peroxides, and aldehydes. The second group consists mostly of newer compounds that leave long-acting residues on the surface to be disinfected and thus have a prolonged action, for example triclosan, triclocarban, and benzalkonium chloride. (APUA, Alliance for the Prudent Use of Antibiotics, 2013)

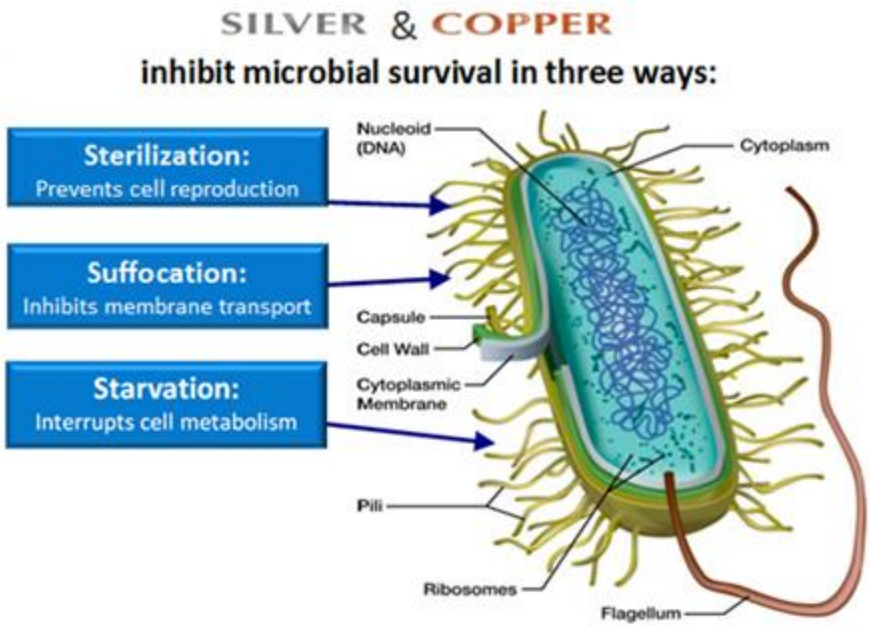

Figure 2.5 : Three ways of silver and copper inhibit microbial survival (Fosshield® fiber manufactured by Foss Manufacturing, LLC)

Antibacterial agents are considered to be relatively non-toxic and they are useful where the level of sanitation is critical and additional precautions need to be taken to prevent spread of disease. Thus, they are important in hospitals, day care centers and healthcare facilities and other environments with high concentrations of infectious bacteria.

Antibacterial silver: The antibacterial properties of silver have been known to cultures all around the world for many centuries. Silver ions and silver compounds show a toxic effect on some bacteria, viruses, algae and fungi without high toxicity to humans. Its germicidal effects kills many microbial organisms in vitro. The Phonecians stored water and other liquids in silver coated bottles to discourage contamination by microbes. Silver dollars used to be put into milk bottles to keep milk fresh, and water tanks of ships and airplanes that are "silvered" are able to render water potable for months (Salt Lake Metals, 2013). In 1884 it became a common practice to administer drops of aqueous silver nitrate to newborn's eyes to prevent the transmission of *Neisseria gonorrhoeae* from infected mothers to children during childbirth (Silvestry-Rodriguez et al., 2007).

In 1893, the antibacterial effectiveness of various metals such as mercury, silver, copper, iron, lead, zinc, bismuth, gold, aluminium, and etc. to living cells, algae, molds, spores, fungi, viruses, prokaryotic and eukaryotic microorganisms, even in relatively low concentrations were noted and this property was named the oligodynamic effect. It was later found that out of all the metals with antimicrobial properties, silver has the most effective antibacterial action and the least toxicity to animal cells (Guggenbichler et al., 1999). Silver became commonly used in medical treatments, such as those of wounded soldiers in World War I. (Saltlakemetals.com). Once antibiotics were discovered, the use of silver as a bactericidal agent decreased. However, with the discovery of antibiotics, the antibiotic-resistant strains such as Methicillin-Resistant *Staphylococcus aureus* (MRSA) are increased. Thus using silver as an antibacterial agent became popular again.

The availability of new laboratory technologies such as radioactive isotopes and electron microscopy has greatly enabled us to investigate the antibacterial mechanism of silver in recent years (Fox and Modak, 1974; Feng et al., 2000). One of the mechanisms how silver inhibits bacterial growth is thought that silver atoms bind to thiol groups (-SH) in enzymes and subsequently cause the deactivation of enzymes. The other suggestion was Ag^+ enters the cell and intercalates between the purine and pyrimidine base pairs disrupting the hydrogen bonding between the two anti-parallel strands and denaturing the DNA molecule (Klueh et al., 2000). Most of the studies proved that silver entering the cell in order to cause cell damage.

Antibacterial copper: Copper is the humankind's oldest metal, used in coins, jewelry, weapons, and for water transportation. Long before the germ theory of disease was developed, civilizations used copper to kill disease-causing organisms, for example Egyptians (2000 BC) used to purify drinking water and treat wounds , Hippocrates (400 BC) used to treat leg ulcers related to varicose veins and Aztecs used copper oxide and malachite for skin conditions (Michels, 2006).

In the past 10 years studies demonstrated that copper inhibits many microorganisms such *E. coli*, methicillin-resistant *Staphylococcus aureus* (MRSA), *Staphylococcus, Clostridium difficile*, influenza A virus, adenovirus, and fungi (Noyce et al., 2004). Copper inhibits *Actinomucor elegans, Aspergillus niger, Bacterium linens, Bacillus megaterium, Bacillus subtilis, Brevibacterium erythrogenes, Candida utilis, Penicillium chrysogenum, Rhizopus niveus, Saccharomyces mandshuricus, and Saccharomyces cerevisiae* in concentrations above 10 g/L (Change et al., 1969). Other studies revealed the molecular mechanisms of antibacterial properties of copper, for example copper complexes form radicals that inactivate viruses (Kuwahara et al., 1982; Vasudevachari, 1982), copper may also facilitates deleterious activity in superoxide radicals. Repeated redox reactions on site-specific macromolecules generate OH- radicals, thereby causing "multiple hit damage" at target sites (Samuni et al., 1984; Samuni et al., 1986).

Copper may interact with lipids, causing their peroxidation and opening holes in the cell membranes, thereby compromising the integrity of cells (Manzl et al., 2004) Copper may disrupt enzyme structures, and functions by binding to sulfur- or carboxylate-containing groups and amino groups of proteins (Sterritt and Lester, 1980). Researchers believe that excess copper has the potential to disrupt cell function both inside cells and in the interstitial spaces between cells, probably acting on the cells' outer envelope. The surfaces of copper and its alloys, such as brass and bronze, are proved to be antimicrobial. Antimicrobial copper-alloy touch surfaces are used in healthcare facilities, where harmful viruses, bacteria, and fungi colonize and persist on doorknobs, push plates, railings, tray tables, faucet handles, IV poles, HVAC systems, and other equipment.

Some antibacterial agents act as killing microorganisms, where others prevent organisms from growing or reproducing. The development of innovative materials with the ability to inhibit bacterial growth has been of great interest in recent years due to their potential use in several products such as paints, food packages, medical devices, fabrics etc. In these products, metallic ions like Ag^{+}, Zn^{2+}, Cu^{2+} are loaded into carriers matrix mainly by ion exchange to be able to increase antibacterial properties of inorganic materials such as clays, zeolites and other aluminosilicates that are used because of their high surface area, high porosity, high ion exchange and sorptive capacity.

2.3.1. Antibacterial clays and minerals

Antibacterial clays are used in many daily products from soaps, detergents, facial masks to health and skincare products and household cleaners.

Figure 2.6 : Antibacterial clay mask and antibacterial facial scrub with herbal clay some of the daily antibacterial clay based products (Url – 1, Url – 2, Url – 3).

Zeolites were used as carriers of silver (Garza et al., 2000; Gómez et al., 2008) copper and zinc ions (Čík et al., 2001; Ulku et al., 2004) also used for the synthesis of Cu(II)-complexes with thiophene oligomers and polythiophene (Čík et al., 2006). Silver (Magaňa et al., 2008; Malachová et al., 2009 and 2011; Özdemir et al., 2004) and copper (Xia et al., 2005; Hu and Xia, 2006; Zhao et al., 2006) ions were loaded into montmorillonite matrix was reported. The antibacterial behaviour of palygorskite, bentonite and sepiolite exchanged with silver (Zhao et al., 2006; Santos et al., 2011) and copper (Zhao et al., 2006; Cubillo et al., 2006) ions against *E. coli* and *S. aureus* were also described. Surface area and cation exchange capacity of clay can also be altered through many methods like acid or thermal treatment and mechanical grinding (Volzone et al., 2001; Aguzzi et al., 2007).

MMT samples treated with calcination at 550°C for 3h and grinding during 300s., silver ion exchanged samples antibacterial activity against *E. coli*, measured by the disk susceptibility and minimum inhibitory concentration (MIC) tests (Magana et al., 2007).

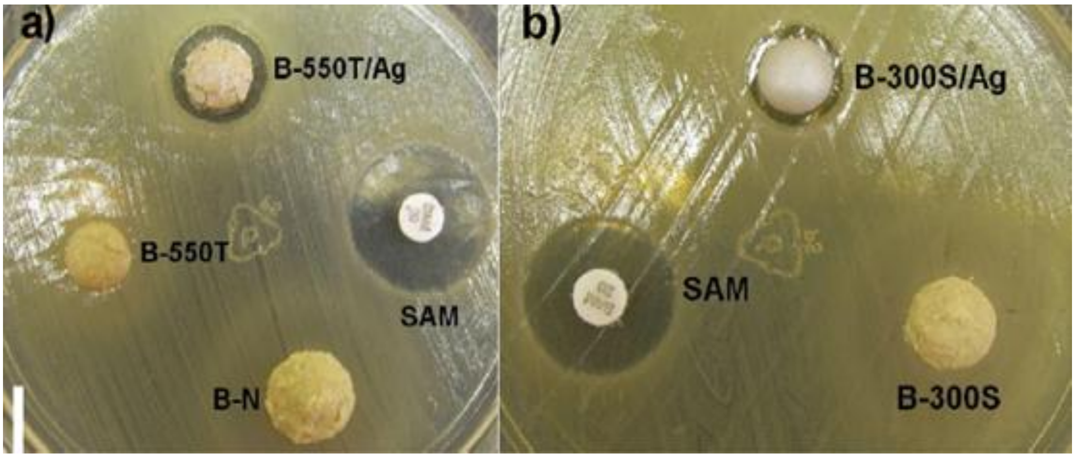

Figure 2.7 : Comparison of the inhibition zone test between the standard antibacterial material (SAM, Ampicilin/Sulbactam) and natural clay (B-N) with: (a) clay calcined at 550°C (B-550T) with and without Ag^+ and (b) ground sample (B-300S) with and without Ag^+ (Magana et al., 2007).

Antibacterial activity of Ag-MMT, Cu-MMT and Zn-MMT samples were investigated against *Escherichia coli* and found in this order: Ag-MMT > Cu-MMT ≈ Zn-MMT (Malachová et al., 2009). Same group also tested silver ions and metallic silver, immobilised on montmorillonite (MMT), in *E. coli* (Malachová, 2008) Cu^{2+} exchanged Calcium montmorillonite (Cu/Ca-MMT), sodium MMT (Cu/Na-MMT) and acid-activated MMT (Cu/AAM), the ranking of antibacterial activity of the three clays against *Escherichia coli* was as Cu/AAM > Cu/Na-MMT > Cu/Ca-MMT (Hu and Xia, 2006). Disk diffusion test is used to measure antibacterial effects of Cu^{2+}-, Zn^{2+}-, Ag^{+}-, Ag^{0}- exchanged montmorillonites on *Staphylococcus aureus* strains which is highly resistant to antibiotics and cause severe infections in hospitalized patients (Ozdemir et al., 2010). Copper monodispersed nanoparticles embedded into sepiolite (Figure 2.8) were able to reduce the *S. aureus* and *E. coli* concentrations by 99.9%, which is identical to the efficacy of Triclosan (Esteban-Cubillo et al., 2006).

Minimum inhibitory concentration (MIC) and zone of inhibition (ZOI) tests were performed to determine Ag^{+} exchanged fluoromicas against *S. aureus* and *E. Coli* (Dizman et al., 2007). Silver and copper modified, acid activated Mingguang palygorskite clays were eliminated the *S. aureus* and *E. Coli* from water within 24h of contact time (Zhao et al., 2006). Raw and acid activated Ag^{+} exchanged bentonite clays also tested against *S. aureus* and *E. Coli* by using agar diffusion and inhibitory concentration minimum methods (Santos et al., 2011). The minimal inhibitory concentration (MIC) of Cu^{2+}-montmorillonite to *E. Coli* was found as 10ppm (Zhou et al., 2004). Montmorillonite (MMT), vermiculite (VER), palygorskite (PAL) and Kaolin (KAO) intercalated by quaternary phosphonium salt (tetradecyl tributyl phosphonium bromide, TDTB) and antimicrobial effects of these clays were tested on *S. aureus* and *E. Coli* with MIC method (Wu et al., 2011). Antibacterial activity of polyethersulfone ultrafiltration membrane containing halloysite nanotubes loaded with copper ions (Cu^{2+}-HNTs/PES) were investigated against *S. aureus* and *E. Coli* by disk diffusion method (Chen et al., 2012). Nanohybrid consists of silver nanoparticles (AgNPs) supported on 1 nm-thick silicate platelets (NSPs) enabled to encapsulate bacteria and triggers death signals from the cell membrane (Figure 2.10) of methicillin resistant *Staphylococcus auerus* and silver-resistant *E. Coli* (Su et al., 2011).

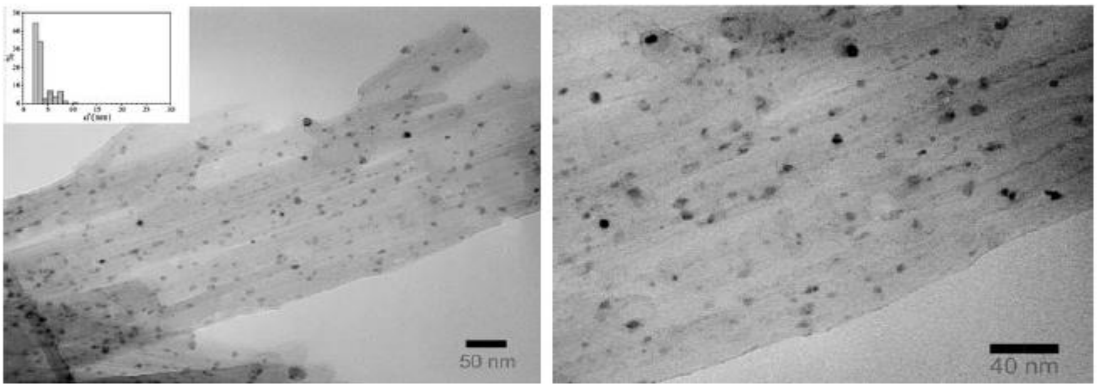

Figure 2.8 : TEM micrographs corresponding to Cu/Sepiolite with their corresponding metal particle size distributions (insets) at two different magnifications (Esteban-Cubillo et al., 2006).

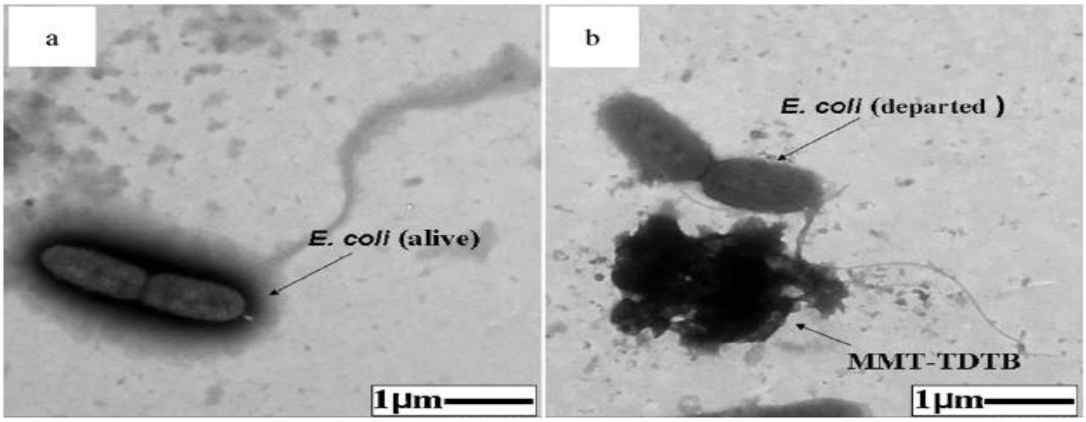

Figure 2.9 : TEM images of normal *E. coli* cells (a) and treated *E. coli* cells by organo-clay minerals (b) (Wu et al., 2011).

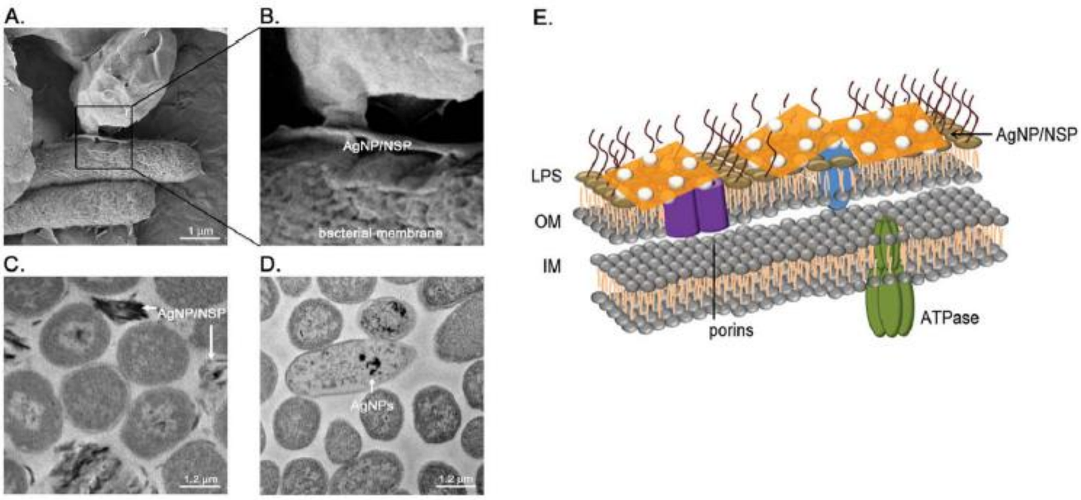

Figure 2.10 : The cell-nanomaterial complexes were examined using FE-SEM (A, B) and TEM (C, D). Nanohybrid-bacteria interaction is illustrated (E). LPS, lipopolysaccharide, OM, outer membrane, IM, inner membrane (Su et al., 2011).

3. MATERIALS AND METHODS

3.1 Material

The raw sepiolite sample consisted of 85±3 % sepiolite was obtained from AEM Co., Turktaciri region of Turkey. The chemical analysis of the sample (Table 3.1) was accomplished with ICP (Inductively Coupled Plasma Spectrometer) in ACME Analytical Lab., Canada. In addition, the mineralogical analysis of the sample (Table 3.2) was also made with Shimadzu XRD-6000 equipped with Cu X-Ray tube (λ= 1.5405 Angstrom). Specific surface area of raw sepiolite sample was analyzed as 222 m2/g using BET surface area by Quanto Chrome Monosorb Analyser (USA).

Table 3.1 : Chemical analysis of the sepiolite sample

Constituent	% by wt
SiO_2	49.85
Al_2O_3	2.38
Fe_2O_3	0.87
MgO	20.15
CaO	2.65
Na_2O	0.10
K_2O	0.36
TiO_2	0.13
LOI	23.5

Table 3.2 : Mineralogical analysis of the sepiolite sample

Mineral Type	Formula
Sepiolite	$Mg_4\,Si_6\,O_{15}\,(OH)_2.6H_2O$
Dolomite	$CaMg\,(CO_3)_2$
Albite	$(Na, Ca)\,Al\,(Si, Al)_3O_8$
Minrecordite	$CaZn\,(CO_3)_2$
Quartz	SiO_2
Calcite	$CaCO_3$
Montmorillonite	$Na0_3(Al, Mg)_2Si_4O_{10}(OH)_2.4H_2O$

XRD results show that the major mineral impurity of Turktaciri region of sepiolite is dolomite along with calcite, albite, quartz, minrecordite and montmorillonite (Table 3.2).

3.2. Atomic Force Microscopy (AFM) Measurements

AFM measurements were performed using XE-70E (Park Systems Corp., Suwon, Korea) in contact mode by NSC36/Cr–Autype cantilevers with 0.5 Hz scanning speed. (AFM,). The AFM measurements were carried out under moisture controlled medium ambient conditions (22 ± 2 °C). Cantilevers were exposed to UV/ozone (UV Cleaner, Bioforce Nanosciences) for 15 min prior to each experiment to remove any possible contamination on each probe. In order to quantify the size of sepiolite fibers on AFM images, all images were processed by XEI Image Processor (Park Systems Corp., Suwon, Korea).

3.2.1. Current-atomic force microscope (I-AFM) measurements

I-AFM is able to image both the topography and the conductivity of the surface at the same time. In I-AFM mode, a conductive AFM tip scans the surface while in contact. The current flows between the tip and the sample allowing I-AFM mode to measure the surface conductivity of a sample. Contact topography image is generated by using feedback loop to maintain the constant tip deflection and I-AFM image is generated by measuring the current flow. In this study, according to semiconductor properties of the samples, two I-AFM modes (Park Systems, 2011) were used: ‘Internal I-AFM’ and ‘External I-AFM’.

3.2.2. Electric force microscopy (EFM) measurements

Electric Force Microscopy (EFM) of the XE-series maps electric properties on a sample surface by measuring the electrostatic force between the surface and a biased AFM cantilever. EFM applies a voltage between the tip and the sample while the cantilever hovers above the surface. EFM images contain information about electric properties such as the surface potential and charge distribution of a sample surface. In this study, using EFM mode of AFM (Park Systems, 2011), electrostatic force between the biased tip and sample was measured as the following procedure: first, the interaction force was changed according to the tip-sample distance. Therefore, electrostatic force was obtained as dominant on the system. Then, the sample was imaged and determined the charge distribution of the sample surface.

Figure 3.1 : AFM (Park System, XE-70E) and its control unit

3.3. Preparation of Silver-nitrate and Copper-sulfate Solutions

To prepare a silver nitrate ($AgNO_3$, Merck) stock solution, 1.5750g of $AgNO_3$ was dissolved in 1000mL of deionized water at room temperature, the solution was protected from sunlight while stirring vigorously for 1h. 1000 mg of Ag^+/L stock solution was then diluted 2-10 fold, the final solution contains 100 mg of Ag^+/L was also diluted to have 1 mg of Ag^+/L.

To prepare a copper sulfate ($CuSO_4.3H_2O$, Merck) stock solution, 3.7980g of $CuSO_4.3H_2O$ was dissolved in 1000mL of deionized water at room temperature, solution was kept from sunlight while stirring vigorously for 1h. This solution contains 1000mg of Cu^{2+}/L. To get necessary volumes stock solution was diluted 2-10 fold, the final solution contains 100mg of Cu^{2+}/L was also diluted to have 1mg of Cu^{2+}/L.

3.4. Adsorption Studies and Preparation of Ag^+- and Cu^{2+}-exchanged Sepiolite Samples

Ag^+- and Cu^{2+}-exchanged sepiolites were prepared by dispersing 2g of raw-sepiolite in 1000mL of 1mg/L - 500mg/L $AgNO_3$ solutions. Both solutions were kept at room temperature and protected from sunlight while stirring vigorously for 24h. All sepiolite dispersions were centrifuged, the sediment was washed with distilled water five times, dried at 80°C overnight and then ground into fine powder. For determination of the metal ion concentration, supernatants were analysed by flame atomic absorption spectrometry (AAS, Perkin).

The adsorbed Ag^{+} and Cu^{2+} ion amount (q_e) per unit absorbent mass was calculated as follows:

$$q_e = \frac{(C_o - C_e)V}{m}$$

where C_o is the initial ion concentration, C_e is the concentration of ions at equilibrium (mg/L), m is the clay mass (mg) and V is the solution volume (L). Calculations were made by using these data and adsorption curves were obtained.

Langmuir isotherm : The Langmuir isotherm is based on these assumptions metal ions are chemically adsorbed at a fixed number of well defined sites; each site can hold only one ion; all sites are energetically equivalent and; there is no interaction between the ions (Langmuir, 1918). Langmuir model can be described by the equation:

$$Q_e = (q_{max}\, b\, C_e)/(1 + b\, C_e)$$

where Q_e and C_e are equilibrium concentrations of adsorbate on adsorbent surface and adsorbate concentration in a solution, respectively. The constant b is related to the equilibrium constant, which represents the affinity between adsorbate and adsobent and q_{max} is the maximum amount adsorbed on the surface (Chong et al., 1995).

When the initial metal concentration rises, adsorption increases while the binding sites are not saturated. The linearized Langmuir isotherm allows the calculation of adsorption capacities and the Langmuir constants and its equated by the following equation.

$$C_e/Q_e = 1/q_{max}\, b + Ce/q_{max}$$

From the linear plots of C_e/Q_e vs Ce, the linear regression equations for the Langmuir isotherm was calculated. From these regression equations and the linear plots, the values of the Langmuir constants were calculated and shown on Table 4.3 q_{max} and b were obtained from the slope and intercept of the plots.

Freundlich isotherm : Freudlich isotherm is strictly an empirical model. Unlike Langmuir model, it does not manifest saturation of adsorbent surface. The sorbed amount increases indefinitely with the concentration in the solution.

The absorbent concentration is a power function of the adsorbate concentration as follows. It is represented by the equation (Freundlich, 1907).

$$Q_e = K_F\, C_e^{1/n}$$

Where C_e is the equilibrium concentration (mg/l), Q_e is the amount adsorbed (mg/g) and K_F and n are constants incorporating all parameters affecting the adsorption process, such as adsorption capacity and intensity respectively. The linearised form of Freundlich adsorption isotherm was used to evaluate the sorption data and is represented as (Ahalya et al., 2005).

$$\ln Q_e = \ln K_F + 1/n \ln C_e$$

The values of K_F and n were calculated from the intercepts and slopes of the Freundlich plots respectively and are shown on Table 4.3.

3.5. Preparation of Luria-Bertani Broth and LB Agar Plates

25g of Luria-Bertani Broth (Powder, Merck) was added into 1000mL of deionized water at room temperature and stirred vigorously for 30 minutes to dissolve equally. 500ml of this solution was transferred to autoclavable glass bottles, for preparing LB Agar 15gr. of Agar agar (Powder, Merck) was added into the other half of the solution and stirred 30 minutes more. After agar dissolved completely, the rest of the solution was transferred into autoclavable glass bottles. Bottles were autoclaved (Nüve OT 100V) at 1,5atm, 121°C for 20 minutes and then cooled to 50°C. For the antibacterial activity measurements, 15mL of LB agar was poured in plates to solidify.

3.6. Growth of Microorganisms

Escherichia coli (ATCC 25922) and *Staphylococcus aureus* (ATCC 25923) were purchased from Center for Culture Collections and Microorganisms, Istanbul Faculty of Medicine, Turkey. Luria-Bertani broth (LB, Merck) was used as a growth medium. Bacterial suspensions were prepared by growing the bacteria overnight at 37°C in LB broth (20mL). The bacterial suspensions were diluted with a sterile saline solution to a final concentration of 1.5×10^8 CFU/mL (0.5 McFarland turbidity).

3.7. Antibacterial Susceptibility Testing Methods

A number of antibacterial susceptibility testing methods are available to determine bacterial susceptibility to antibacterials. Some methods provide quantitative results (eg, Agar, Broth or Serial Dilution Method) and some other methods provide qualitative results (eg, Disk Diffusion). Dilution methods are used to determine the lowest concentration of an antibacterial agent that will inhibit the visible growth of a microorganism is known as the minimum inhibitory concentration (MIC).

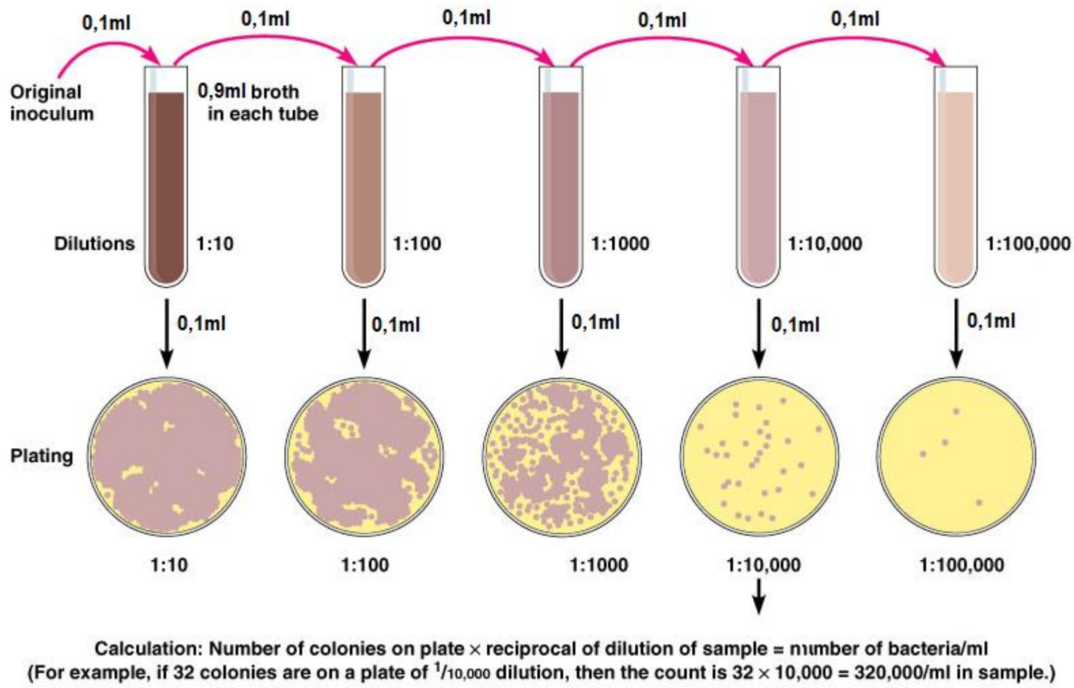

Figure 3.2 : Serial Dilution method is used to determine minimum inhibitory concentration (Cummings, 2004).

3.7.1. Determination of antibacterial activity by serial dilution method

50ml of the each bacterial inoculum was adjusted according to 0.5 McFarland turbidity. 18ml of sterile LB broth and 2ml of the each bacterial inoculum were poured into sterilized plastic tube, respectively. Then, 0.2g of sepiolite samples were added into the tubes. Tubes were placed in the 300 rpm of shaking incubator (Edmund Bühler TH 15) for an overnight incubation at 37°C. Then, tubes were collected and centrifuged for 10 minutes at 10.000 rpm. Later, supernatant was removed by sterile pasteur pipette.

For dilution test 1ml sterile plastic tubes were used. 0.9mL of sterile saline solution was poured into each tube. Later, 0.1mL of the selected aliquot was also added into the first tube. At each step, 0.1mL of the previous dilution was added to 0.9mL of sterile saline solution. Each step results in a further 10-fold change in the concentration from the previous concentration. After dilution, 0.1mL of selected dilutions were inoculated on the surface of LB agar. Then all mediums were incubated at 37°C overnight. After incubation, the bacterial growth was observed. The lowest concentration of antibacterial agent that inhibits visible growth by the naked eye, disregarding a single colony or a thin haze within the surface of agar is taken as minimum inhibitory concentration (MIC).

3.7.2. Determination of antibacterial activity by disk diffusion method

Because of efficiency and cost, the disk diffusion method is probably the most widely used method for determining antibacterial susceptibility. Antibacterial activity of the raw, Ag^{+} and Cu^{2+}-exchanged sepiolites were tested on *E.coli* and *S.aureus*. 0.1mL of the each bacteria suspension adjusted to 0.5 McFarland turbidity was used to inoculate the surface of LB agar plate. By the use of a drigalski-spatula bacterial suspension was homogeneously spread on agar plates. On the other hand, 0.2g of the sepiolite samples, were separately pressed into pellets (7mm diameter) and placed over the surface of the agar coated plates. Then all plates were incubated at 37°C overnight. The results were also compared with the Ampicillin/sulbactam (SAM) antibiotic discs and control sample of raw sepiolite.

After an overnight incubation, the bacterial growth was observed around each pellets. Inhibition zone is then measured in mm and results compared with control groups (raw sepiolite pellets and antibiotic discs).

4. RESULTS and DISCUSSIONS

4.1. Adsorption Isotherms

Equilibrium relationships between adsorbent and adsorbate are described by adsorption isotherms which are usually the ratio between the quantity adsorbed and the remaining in solution at fixed temperature at equilibrium. Adsorption models of Ag^{+} and Cu^{2+}-exchanged sepiolites were determined through batch experiments.

Table 4.1 : Langmuir and Freundlich model values of Ag^{+} adsorption on sepiolite

2g sepiolite in 1000ml Ag^{+} solution		**Langmuir model values**		**Freundlich model values**	
C_o	**C_e**	**C_e/Q_e**	**Q_e**	**Log C_e**	**Log Q_e**
1	0,01	0,020202	0,495	-2	-0,30539
50	10,7	0,544529	19,65	1,02938	1,29336
100	35,7	1,110419	32,15	1,55266	1,50718
200	100,5	2,020100	49,75	2,00216	1,69679
300	177,6	2,901960	61,2	2,24944	1,78675
400	261,6	3,780346	69,2	2,41763	1,84010
500	388,05	6,932559	55,975	2,58888	1,74799

Table 4.2 : Langmuir and Freundlich model values of Cu^{2+} adsorption on sepiolite

2g sepiolite in 1000ml Cu^{2+} solution		**Langmuir model values**		**Freundlich model values**	
C_o	**C_e**	**C_e/Q_e**	**Q_e**	**Log C_e**	**Log Q_e**
1	0,01	0,020202	0,495	-2	-0,30539
50	9,8	0,487562	20,1	0,9912261	1,303196
100	23,6	0,617801	38,2	1,372912	1,582063
200	51,7	0,697235	74,15	1,7134905	1,870111
300	92,9	0,897151	103,55	1,9680157	2,01515
400	229	2,678363	85,5	2,3598355	1,931966
500	320	3,555556	90	2,50515	1,954243

Figure 4.1 : Linear plots of C_e/Q_e vs Ce (a) and Log $[Q_{e]}$ vs Log [Ce] (b) for the Languir and Freundlich isotherms of Ag^+ adsorption on sepiolite, respectively.

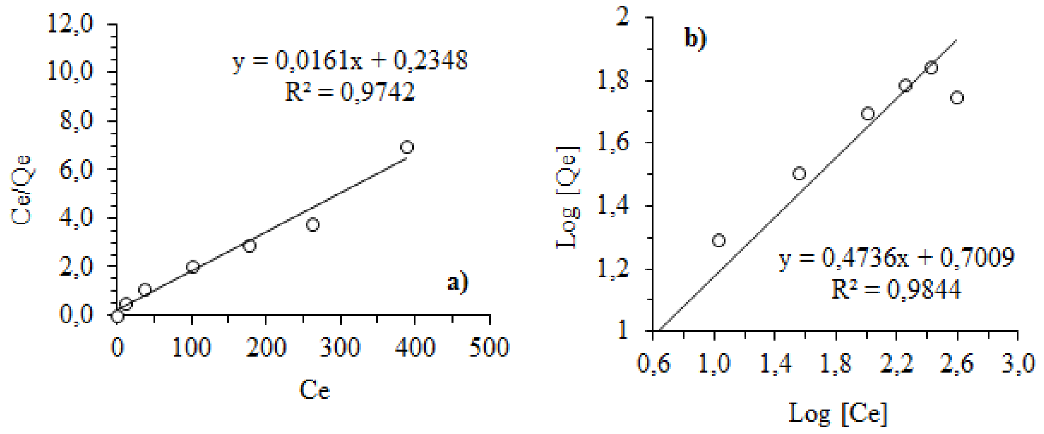

Figure 4.2 : Linear plots of C_e/Q_e vs Ce (a) and Log $[Q_{e]}$ vs Log [Ce] (b) for the Langmuir and Freundlich isotherms of Cu^{2+} adsorption on sepiolite, respectively.

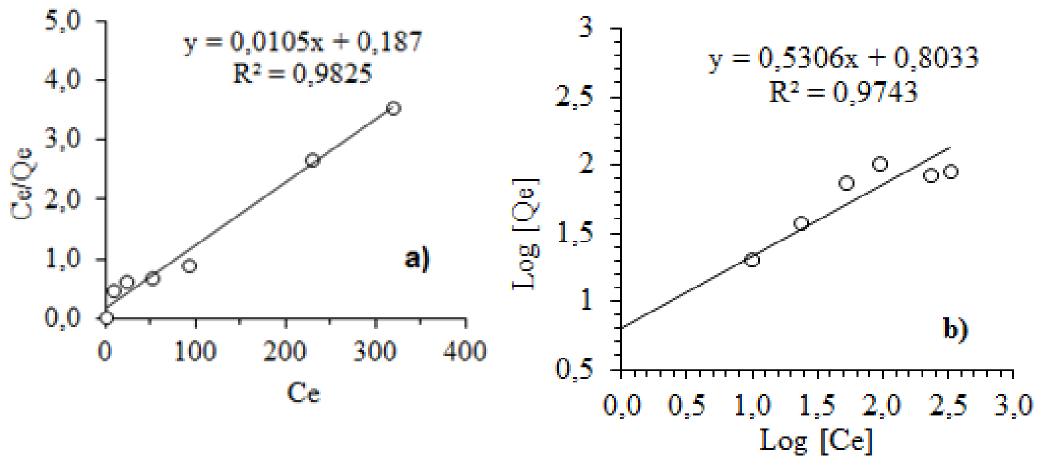

Table 4.3 : Langmuir and Freundlich model constants of Cu^{2+} and Ag^+ adsorption on sepiolite

	Constants	**Cu^{2+} adsorption**	**Ag^+ adsorption**
Langmuir Model	$1/q_{max}$	0,0105	0,0161
	$1/(q_{max}\,b)$	0,187	0,2348
	$q_{max}\,b$	5,34759	4,25894
	q_{max}	95,2381	62,1118
	b	0,05615	0,06857
	R^2	0,98	0.97
Freund-lich Model	K_F	0,8033	0,7009
	1/n	0,5306	0,4736
	R^2	0.97	0,98

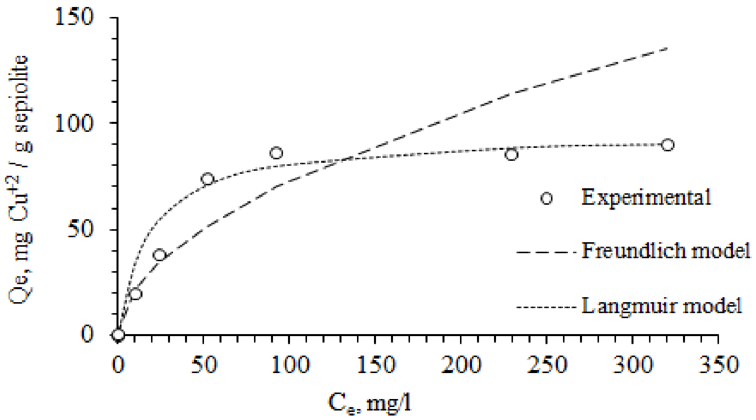

Figure 4.3 : Adsorption isotherm behavior of Ag^{+} ion on sepiolite

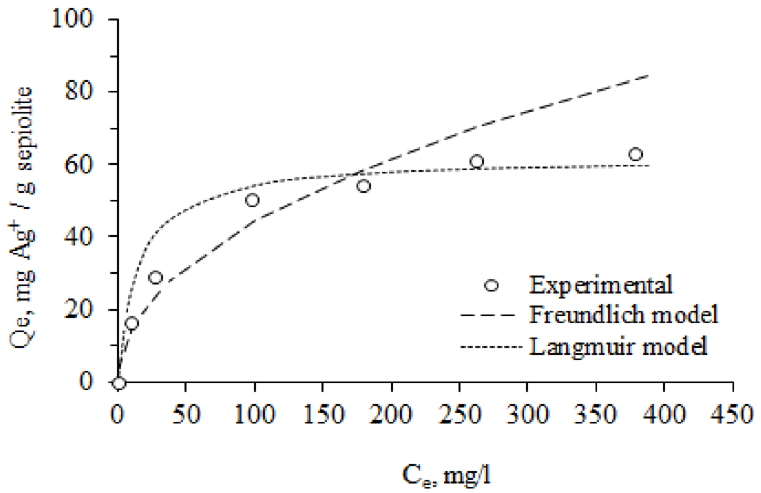

Figure 4.4 : Adsorption isotherm behavior of Cu^{2+} ion on sepiolite

Using the adsorption isotherms, the obtained data were linearized in Fig.4.1 and 4.2. Linear plots were analyzed for the regression coefficients of Langmuir and Freundlich model. According to the adsorption isotherm models of both Ag^{+} and Cu^{2+} adsorption on sepiolite (Figure 4.3; Figure 4.4), Langmuir model was determined as the best fitting model for both Cu^{2+} and Ag^{+} adsorption on sepiolite.

4.1.1. Fourier transform infrared spectroscopy (FTIR) spectra of raw, Cu^{2+} and Ag^{+} - exchanged sepiolite fibers

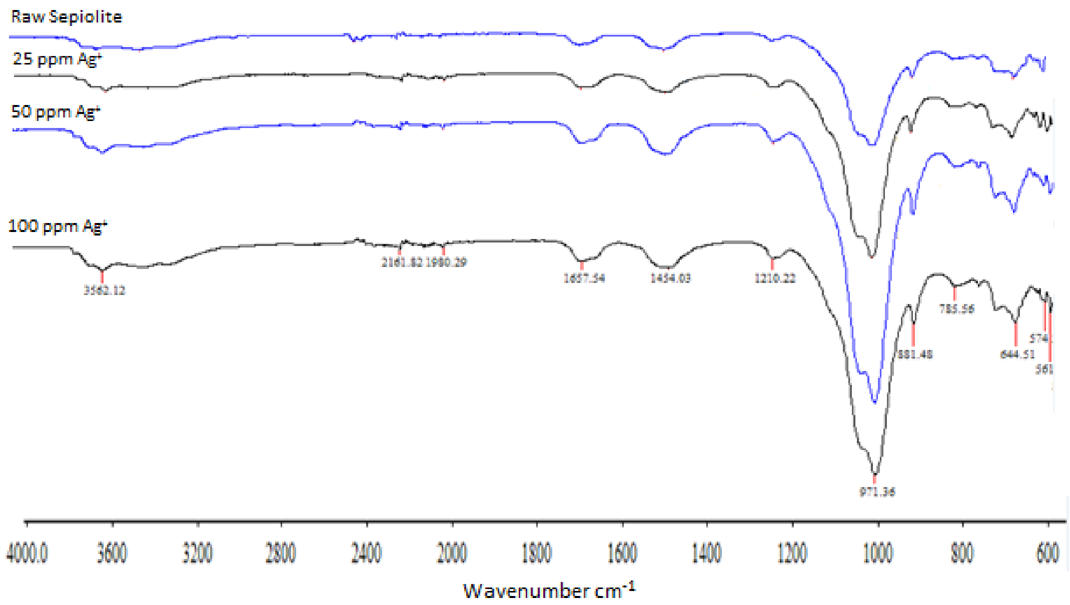

Figure 4.5 : FTIR spectra of the raw sepiolite and Ag^{+} exchanged samples

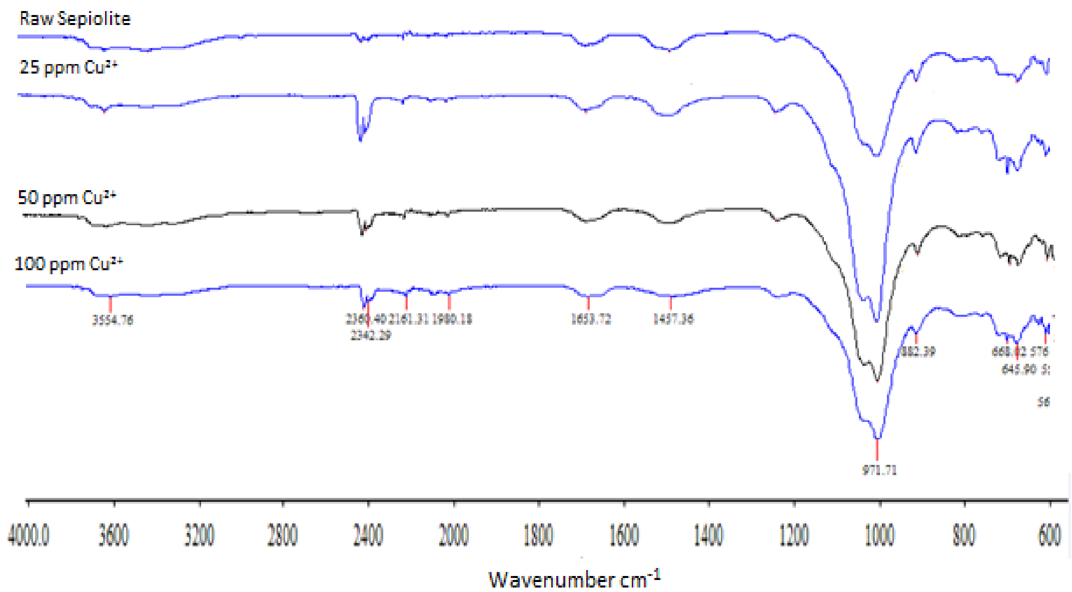

Figure 4.6 : FTIR spectra of the raw sepiolite and Cu^{2+} exchanged samples

Table 4.4 : FTIR results of raw, Cu^{2+} and Ag^{+} exchanged sepiolite fibers

	Wavelenghths cm^{-1}											
25 ppm Ag^{+}	3562.13			2161.62	1980.27	1657.94	1461.47	1210.13	973.56	881.99		644.24
50 ppm Ag^{+}	3555.05			2161.96	1980.45	1657.26	1461.21	1209.86	971.50	881.85	784.92	645.15
100 ppm Ag^{+}	3562.12			2161.82	1980.29	1657.54	1454.03	1210.22	971.36	881.48	785.56	644.51
25 ppm Cu^{2+}	3563.19	2360.36	2341.81	2161.46	1980.10	1653.44	1457.27	1210.72	974.92	882.92	668.07	645.70
50 ppm Cu^{2+}	3562.38	2360.36	2341.83		1980.44	1653.19	1457.24	1210.24	975.31	882.82	668.03	645.94
100 ppm Cu^{2+}	3554.76	2360.40	2342.89	2161.31	1980.18	1653.71	1457.36		971.71	882.39	668.02	645.90
Raw Sepiolite	3562.85	2360.66			1980.28	1653.20	1457.11	1210.09	974.31	880.93		645.69
Treated Raw	3362.05	2360.75				1653.86	1457.92		974.50	881.61		644.81
Sepiolite 1	3562.48	2360.63		2161.79	1980.24	1654.02	1457.71	1209.98	973.44	881.86		644.15
Sepiolite 2	3562.76	2360.31			1980.08	1653.82	1457.47	1209.97	973.48	881.93		643.67

According to the FTIR results of Ag^{+} exchanged sepiolite fibers, the peak at 2360cm^{-1} was disappeared when another peak was appeared at 784cm^{-1} comparing to raw sepiolite fiber results. As for, Cu^{2+} exchanged sepiolite fibers two peaks were appeared at 2341cm^{-1} and 668cm^{-1} where both of these peaks were not observed for raw sepiolite fibers.

4.2. Antibacterial Activity of Cu^{2+} and Ag^{+} Exchanged Sepiolite Fibers

The results of disk diffusion tests showed that silver ions are stronger antibacterial agents than copper ions where raw samples show no antibacterial activity. Also, Gram negative bacteria *E.Coli* is more resistant to silver and copper ions than *S. aureus.*

In serial dilution method, different concentrations of silver and copper exhanged sepiolite sample were tested against both microorganisms. After an overnight incubation, all colonies per plate were counted. To calculate the final number of bacteria (CFU/ml), counted number of colonies multiply by the dilution factor (Figure 4.7). The lowest concentration of antibacterial agent that inhibits visible growth as observed by the naked eye, disregarding a single colony or a thin haze within the surface of agar is taken as minimum inhibitory concentration (MIC). 50mg/L and 100mg/L were determined as the minimum inhibitory concentration for the silver and copper exchanged sepiolite fibers, respectively.

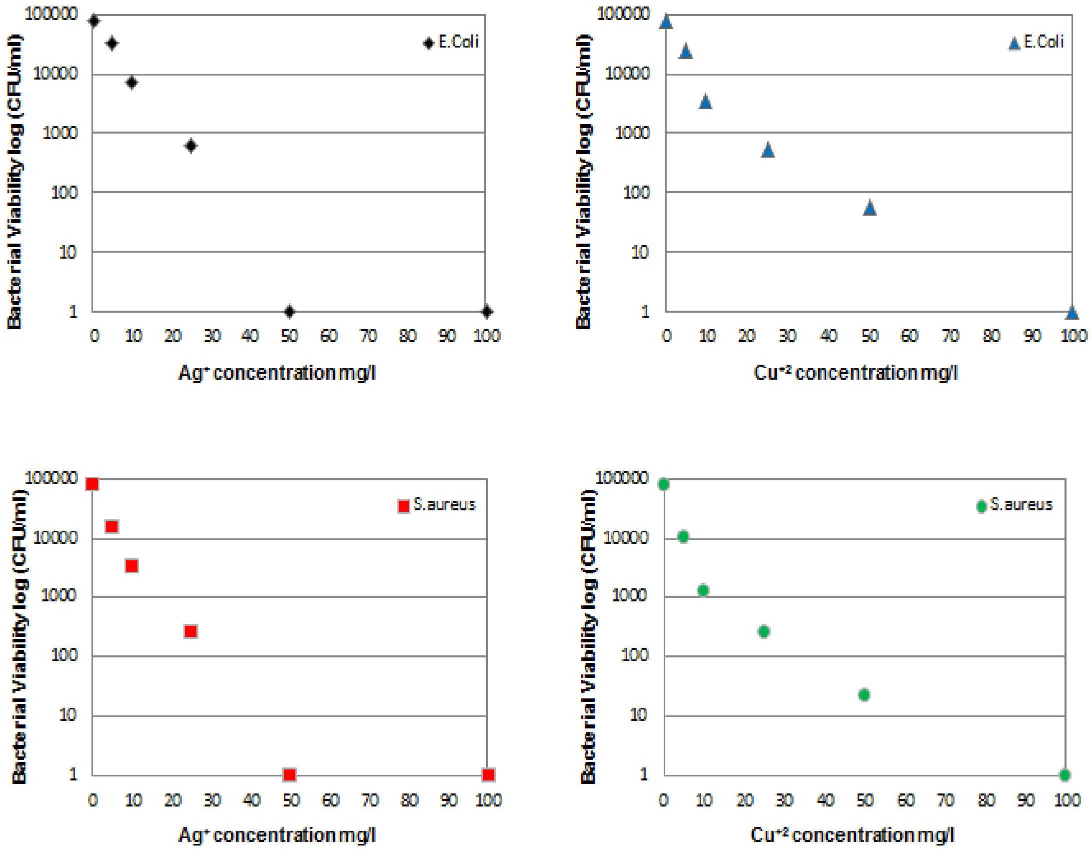

Figure 4.7 : Bacterial viability of two different bacteria strains (*E.Coli* and *S.aureus)* against Ag^{+} and Cu^{2+} concentration of ion exchanged sepiolite samples. According to the calculations, 50mg/L and 100mg/L were determined as the minimum inhibitory concentration of Ag^{+} and Cu^{2+} exchanged sepiolite fibers, respectively.

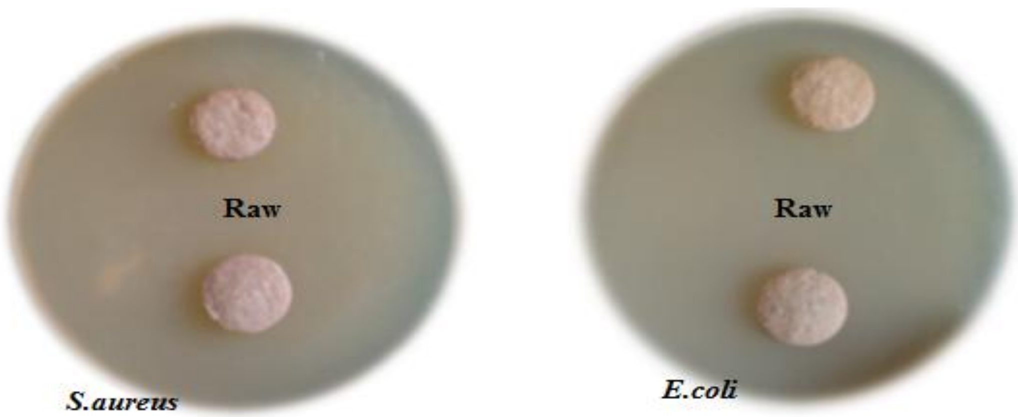

Figure 4.8 : Mozley table separated (raw) sepiolite disks were used as control groups and they showed no antibacterial activity.

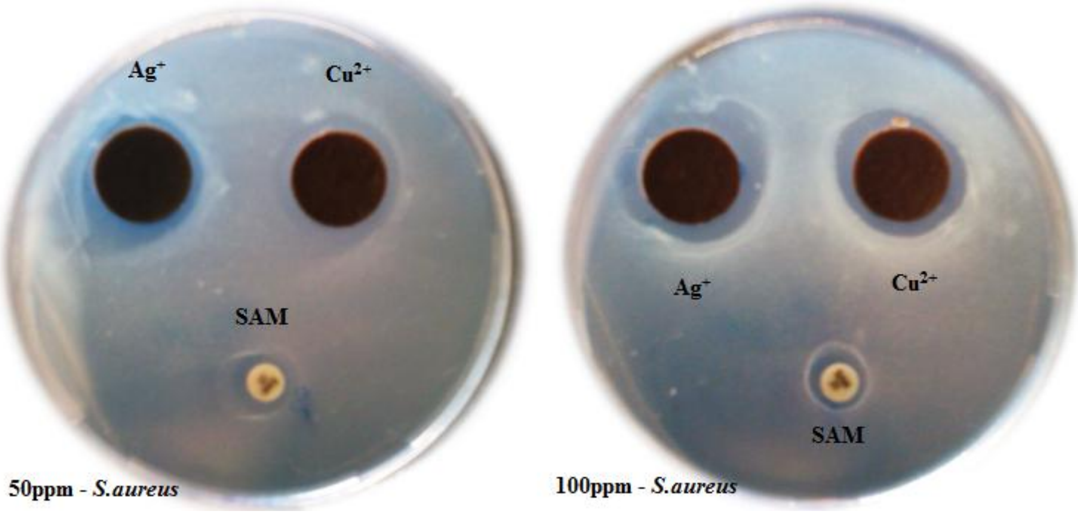

Figure 4.9 : Antibacterial activity of 50ppm and 100ppm Cu^{2+} and Ag^{+} exchanged sepiolite disks against *S.aureus.* 100ppm Cu^{2+} and Ag^{+} exchanged samples showed better antibacterial activity than 50ppm Cu^{2+} and Ag^{+} loaded samples. SAM (ampicilin/sulbactam) antibiotic disks used as control group.

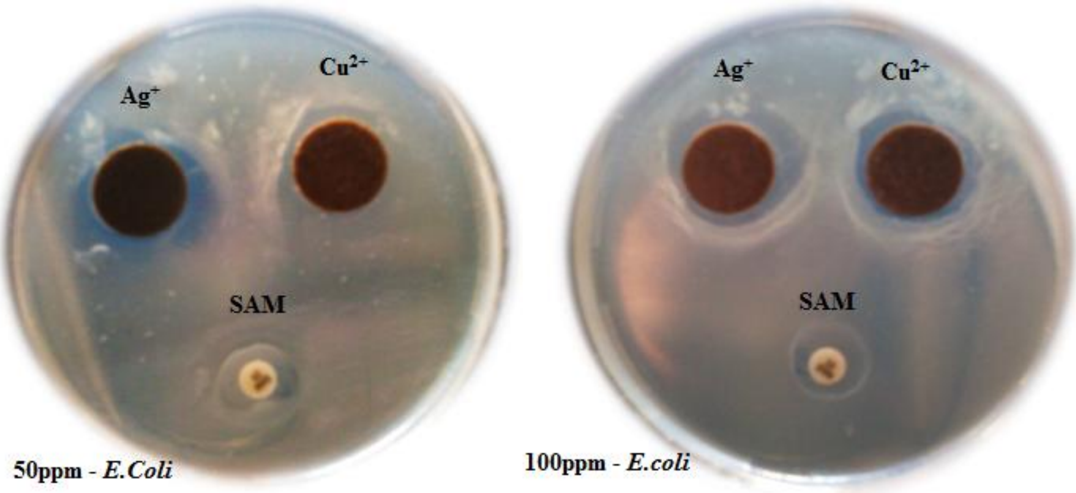

Figure 4.10 : Antibacterial activity of 50ppm and 100ppm Cu^{2+} and Ag^{+} exchanged sepiolite disks against *E.coli.* 50ppm Cu^{2+} loaded sepiolite samples showed weak antibacterial activity where 50ppm Ag^{+} loaded sample almost has same antibacterial activity as 100ppm Ag^{+} loaded samples.

It had been shown that the charge of these modified clays with Ag^{+} or Cu^{2+} ions may enhance their ability to attract bacteria through electrostatic and hydrophobic interactions (Liau et al., 1997; Kawahara et al., 2000).

Table 4.5 : Kirby-Bauer disk diffusion susceptibility test results of various type of clays tested on *E.Coli* and *S.aureus* microorganisms

Study	**Type of Clay**	**Exchanged Ion**	**Bacteria Strain**	**Initial diameter (mm)**	**Final inhibition zone diameter (mm)**
Magana et al., 2007	MMT-550T (calcination 550 ◦C)	$AgNO_3$	*E.Coli*	7	13.3
Magana et al., 2007	MMT-300S (mechanical grinding)	$AgNO_3$	*E.Coli*	7	12.3
Santos et al., 2011	HCl-activated bentonite	$AgNO_3$	*E.coli* *S.aureus*	-	+1.5 +3.5
Santos et al., 2011	Raw bentonite	$AgNO_3$	*E.coli* *S.aureus*	-	+1.5 +2.5
Özdemir et al., 2010	MMT	Cu^{2+} Zn^{2+} Ag^{+} Ag^{0}	*S.aureus*	-	18 22 20 20
Dizman et al., 2007	Fluoromica clay	Ag^{+}	*E.coli* *S.aureus*	8	11
Chen et al., 2012	Halloysite	Cu^{2+}	*E.coli* *S.aureus*	10 9	15 12
In this study	SAM (ampicilin/ sulbactam)	-	*E.coli* *S.aureus*	2.5	7 9
	Sepiolite	Raw	*E.coli* *S.aureus*	7	7 7
	Sepiolite	Ag^{+} (100ppm)	*E.coli* *S.aureus*	7	12 13
	Sepiolite	Cu^{2+} (100ppm)	*E.coli* *S.aureus*	7	10 11

Table 4.6 : Minimum inhibitory concentration values of various type of clays tested on *E.Coli* and *S.aureus* microorganisms

Study	Type of Clay	Exchanged Ion	Bacteria Strain	MIC
Santos et al., 2011	HCl-activated bentonite	$AgNO_3$	*E.coli* *S.aureus*	12mg 22mg
Santos et al., 2011	H_2SO_4-treated bentonite	$AgNO_3$	*E.coli* *S.aureus*	38mg 38mg
Magana et al., 2007	MMT-550T (calcination 550 ◦C)	$AgNO_3$	*E.Coli*	2.5mg
Magana et al., 2007	MMT-300S (mechanical grinding)	$AgNO_3$	*E.Coli*	1mg
Dizman et al., 2007	Fluoromica Clay	Ag^{+1}	*E.coli* *S.aureus*	5mg/mL
Zhao et al., 2006	Acid activated Mingguang palygorskite	$AgNO_3$ $Cu(NO_3)_2$	*E.coli* *S.aureus*	1mg/mL 1mg/mL
Zhou et al., 2004	MMT	$CuSO_4$	*E.coli*	10mg/L
Wu et al. 2012	MMT KAO	Quaternary phosphonium salt (TDTB)	*E.coli* *S.aureus*	200mg/L 80mg/L
Wu et al. 2012	PAL	TDTB	*E.coli* *S.aureus*	800mg/L 150mg/L
In this study	Sepiolite	Ag^{+}	*E.coli* *S.aureus*	50mg/L 50mg/L
	Sepiolite	Cu^{2+}	*E.coli* *S.aureus*	100mg/L 100mg/L

Under physiologic conditions, bacterial cell walls are negatively charged due to functional groups such as carboxylates present in lipoproteins at the surface and exhibit a net negative charge. *E. coli*, is a gram-negative bacterium with an outer membrane (OM) covering a thin layer of peptidoglycan, which provides E. coli with a hydrophilic surface and functions as a permeability barrier for many external agents.

Since the peptidoglycan layer of Gram positive bacteria is much thicker than the negative ones. Gram positive bacterias attract more positive ions and they are more vulnerable to attack of antibacterial agents as seen in Figure 4.11.

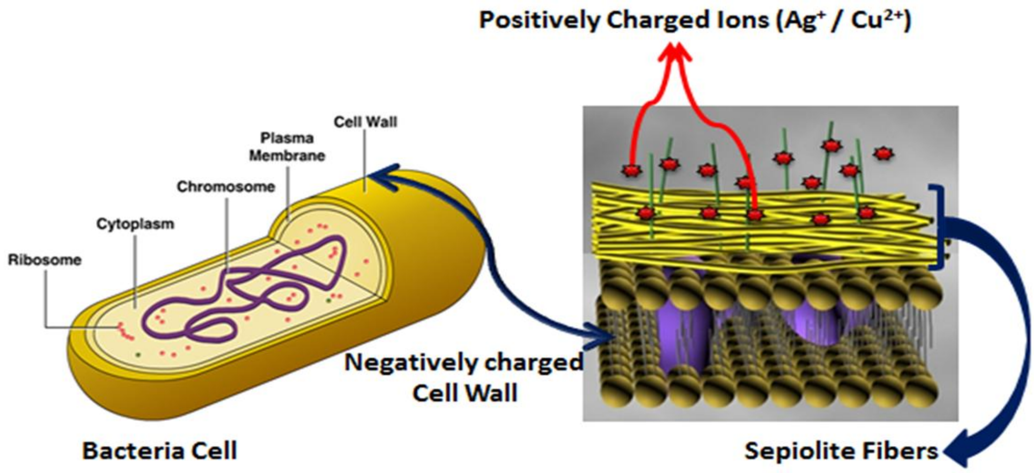

Figure 4.11 : The schematic illustrations for sepiolite fibers and bacteria cell interaction (Url – 4).

Ag^+ ions are known to induce numerous damages in G+ and G− bacterial cells. Ag^+ easily penetrates through the cell wall and cytoplasmic membrane inside the bacterial cell. The binding of Ag^+ to thiol (SH) groups in the cytoplasm inactivates enzymes, which subsequently causes various metabolic damages and reduce the vitality (Gajjar et al., 2009; Feng et al., 2000) studied morphological changes of *E. coli* cells by Ag^+. Large gaps between the cytoplasmic membrane and the cell wall were observed by TEM as well as the condensation of big granules and DNA molecules leading to a loss of the replication ability.

The Cu^{2+} exhanged clays also attracted the bacteria by electrostatic forces. Inactivation of bacteria by Cu^{2+} exhanged clays may involve killing the bacteria or merely rendering them unable to replicate. Besides, due to the density of the Cu^{2+}

ions on the mineral surface much higher than that in the solution, the antibacterial activity of Cu-clay particles might dominate over the Cu^{2+} cations released into the medium. Therefore, the Cu^{2+} bridging between the montmorillonite particle and the bacteria played an important role. Our present model is that the positive charge of the Cu-MMT brings bacteria in close association to the surface, whereupon the Cu^{2+} ions exert the antibacterial activity (Jung, 2008).

After washing the treated clay samples with distilled water at least five times, the samples maintained their antibacterial activity and were just as effective as the first time in the second trials.

4.3. Electrical Properties of Cu^{2+} and Ag^{+} Loaded Sepiolite Fibers

The surface heterogeneity of sepiolite for a single fiber surface was determined from the AFM images. AFM image shows that sepiolite fiber or bundles produces an area random netweork and assembly of multiple fibers. Red line was measured XEI analysis program and imaged with 200nm of average width and 1 micron of average length for a single fiber in Fig. 4.12 (Wang et al., 2010) also obtained similar sepiolite nanofibers dispersed by jet mill constituted an average diameter of about 100nm and length greater than 9µm.

I-AFM measurements (Fig. 4.13) were performed to indicate electrical conductivity of separated and ion loaded sepiolite samples. I-AFM is able to image both the topography and the conductivity of the surface at the same time.

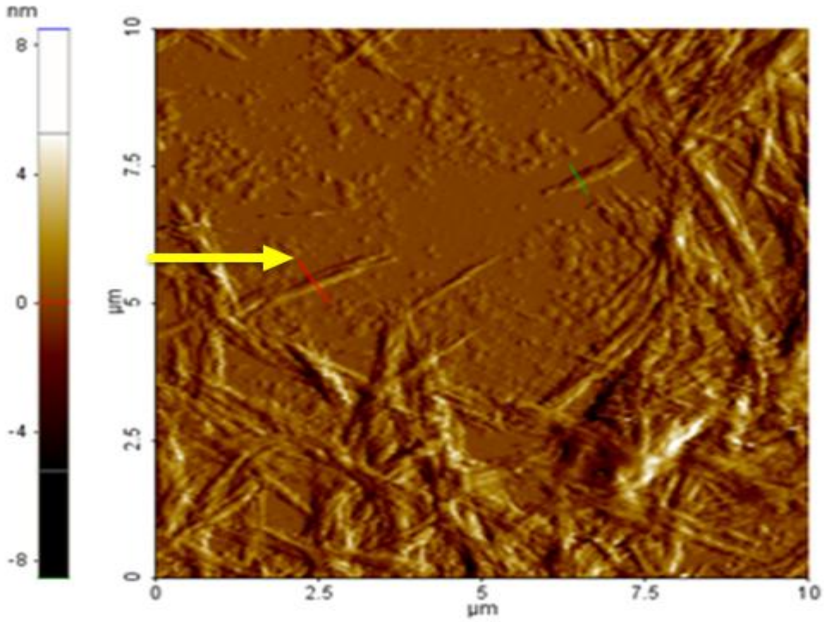

Figure 4.12 : AFM image of a single fibrous sepiolite. Red line is a single sepiolite fiber : 200 nm width x 1 µm length.

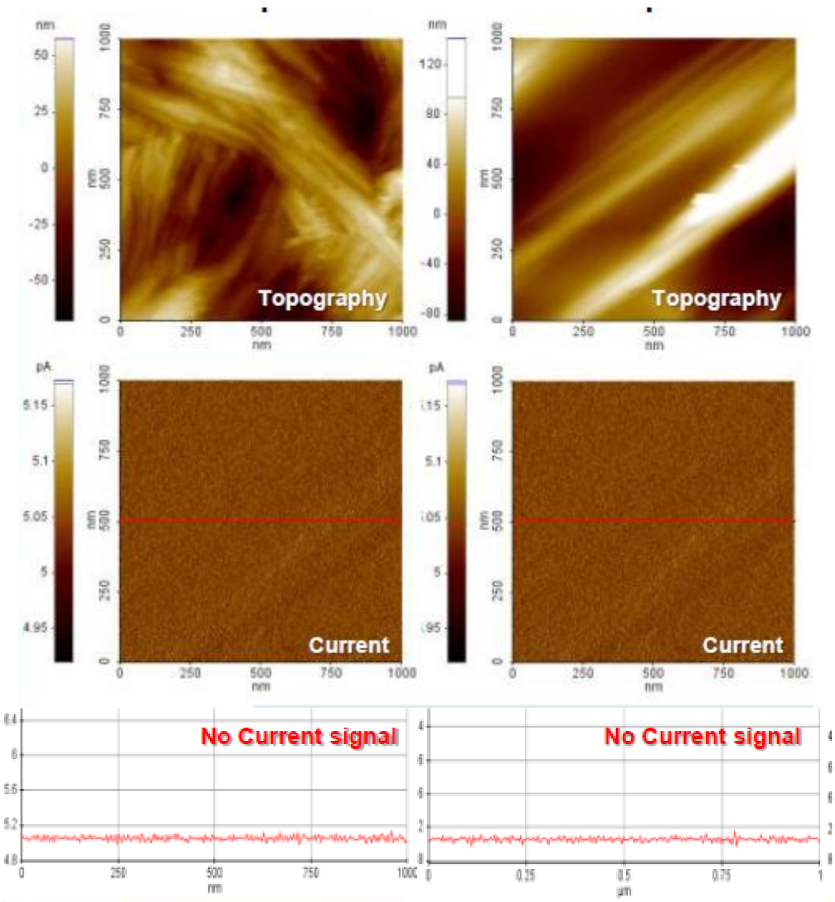

Figure 4.13 : I-AFM electric conductivity measurements of (a) raw sepiolite sepiolite fibers before and (b) after gravity separation. Cantilever: ContscPt(k=0.2N/m)

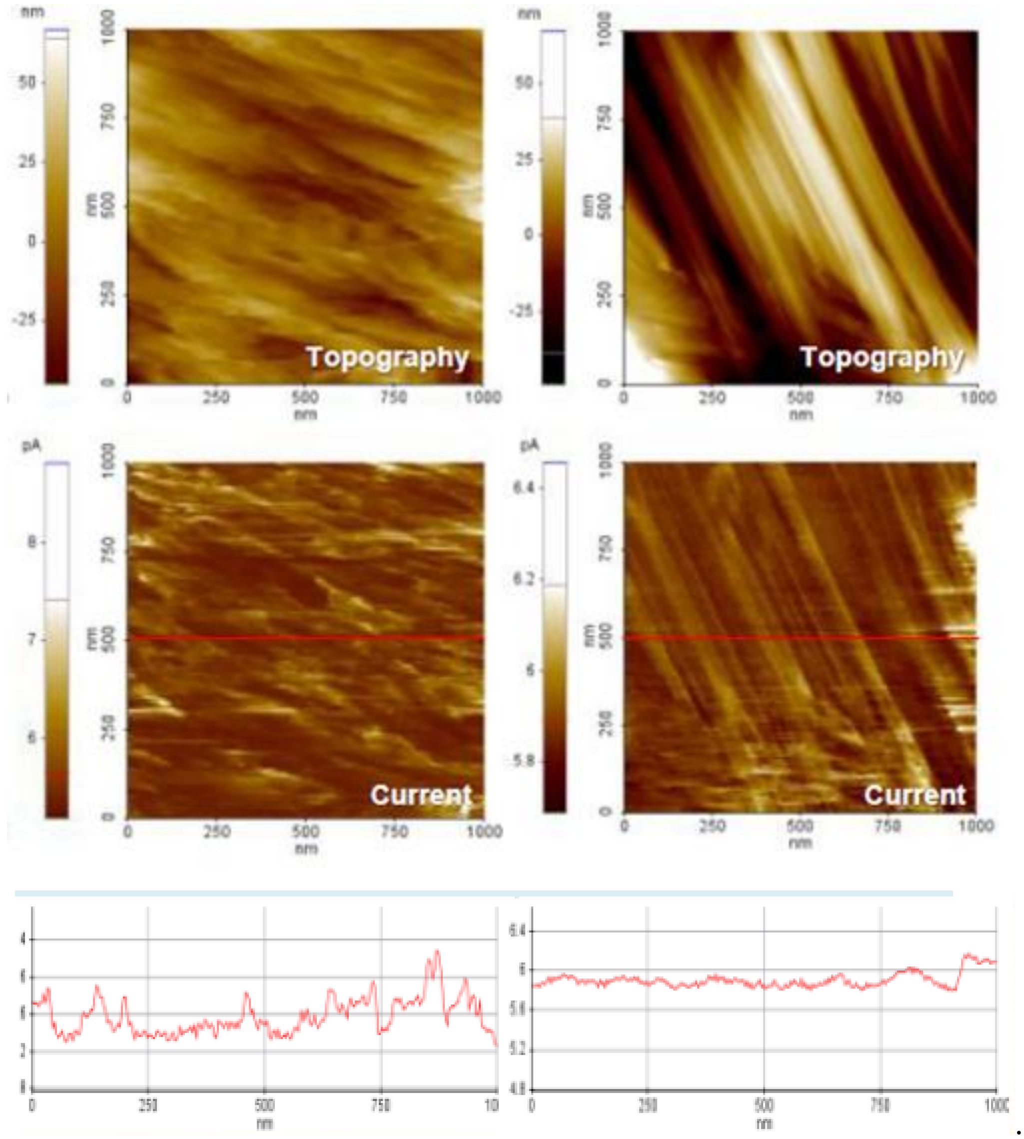

Figure 4.14 : I-AFM electric conductivity measurements of ion loaded sepiolite (a) Ag exchanged fibers, (b) Cu exchanged fibers. Cantilever: ContscPt(k=0.2N/m)

< I-AFM current range >

Internal : 2nA~2μA(current), ~100mA(log current)

External (VECA) : 10pA~10mA

External (ULCA) : 100fA~100pA

With applying different biases, EFM study was also carried out to show electrical properties of sepiolite surfaces.

EFM study was carried out on a 2μm x 2μm area, as 0 bias surface topography was showed for raw and silver or copper exchanged sepiolite fibers. When bias applied, electrostatic forces dominated van der Waals interactions. Between 16.0-17.0nm current range, raw and copper exchanged samples gave current signals. As for silver exchanged sepiolite sample, current range dropped to 15.7nm. These results showed that Ag^+ exchanged sepiolite fibers have better electrical conductivity than copper exchanged samples, and they may be used as nanowires for various applications.

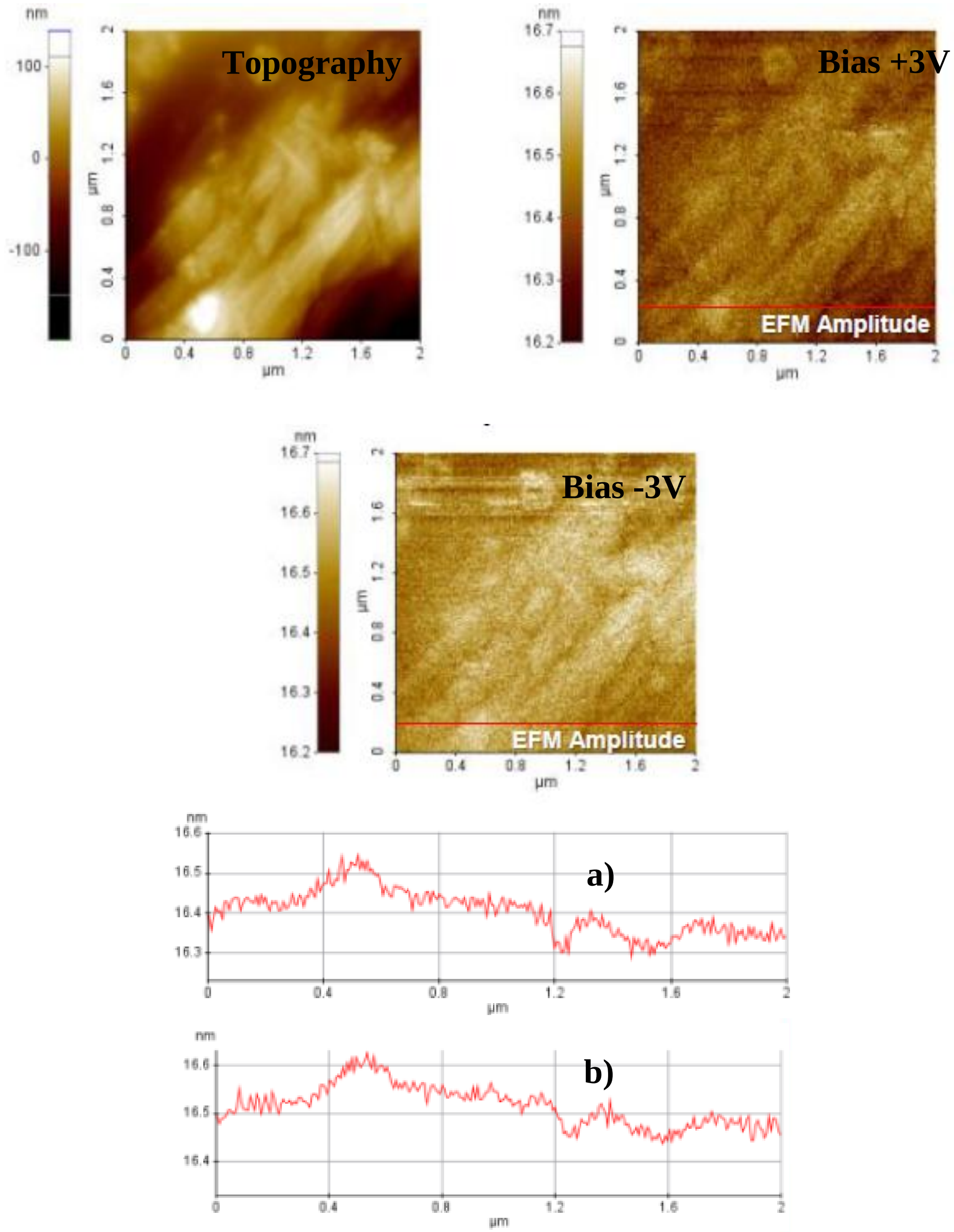

Figure 4.15 : Current signals of raw samples measured with Internal EFM, (a) +3V Bias, (b) -3V bias

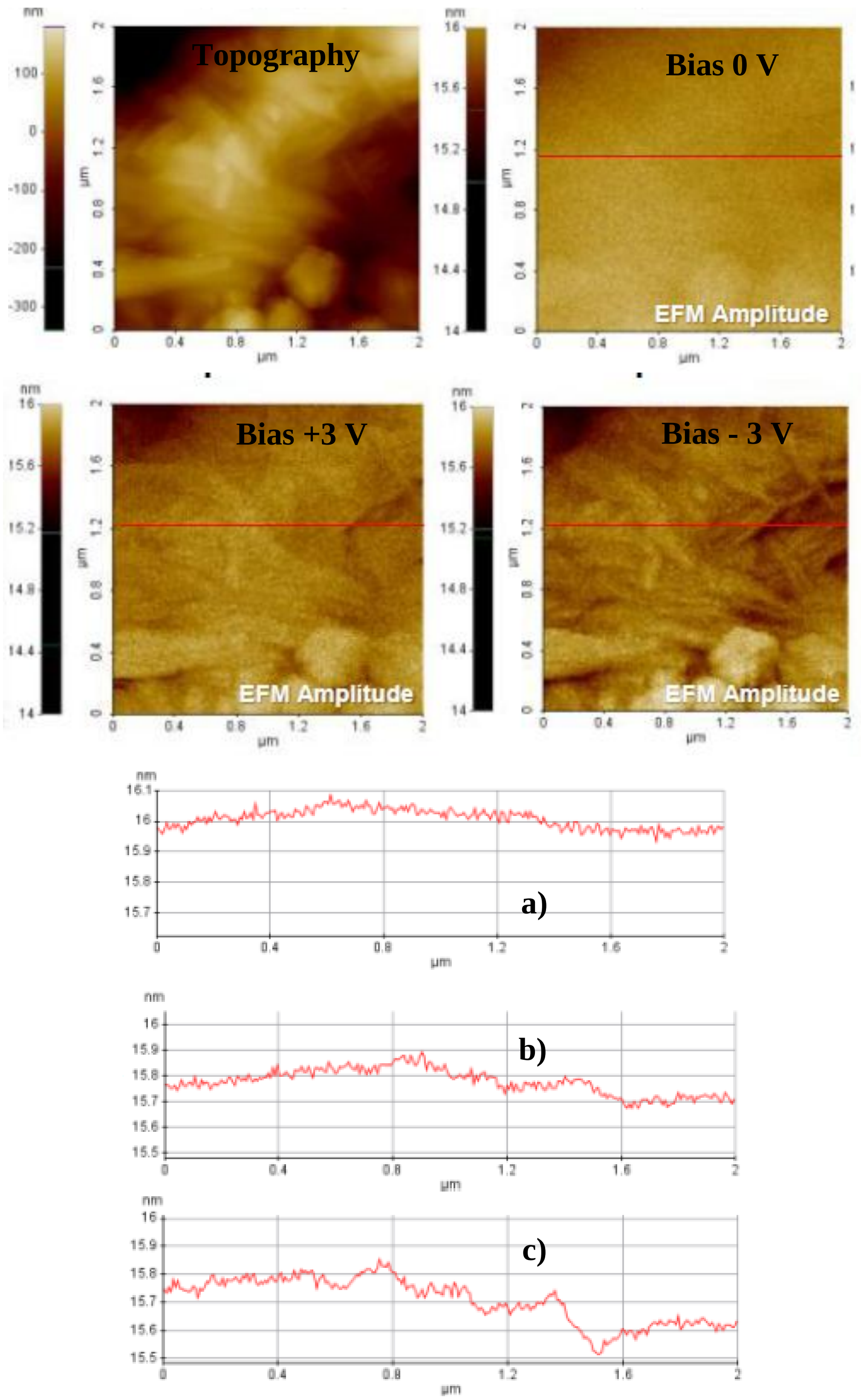

Figure 4.16 : Current signals of Ag^{+} exchanged samples measured with Internal EFM (a) 0 Bias, (b) +3V Bias, (c) -3V bias

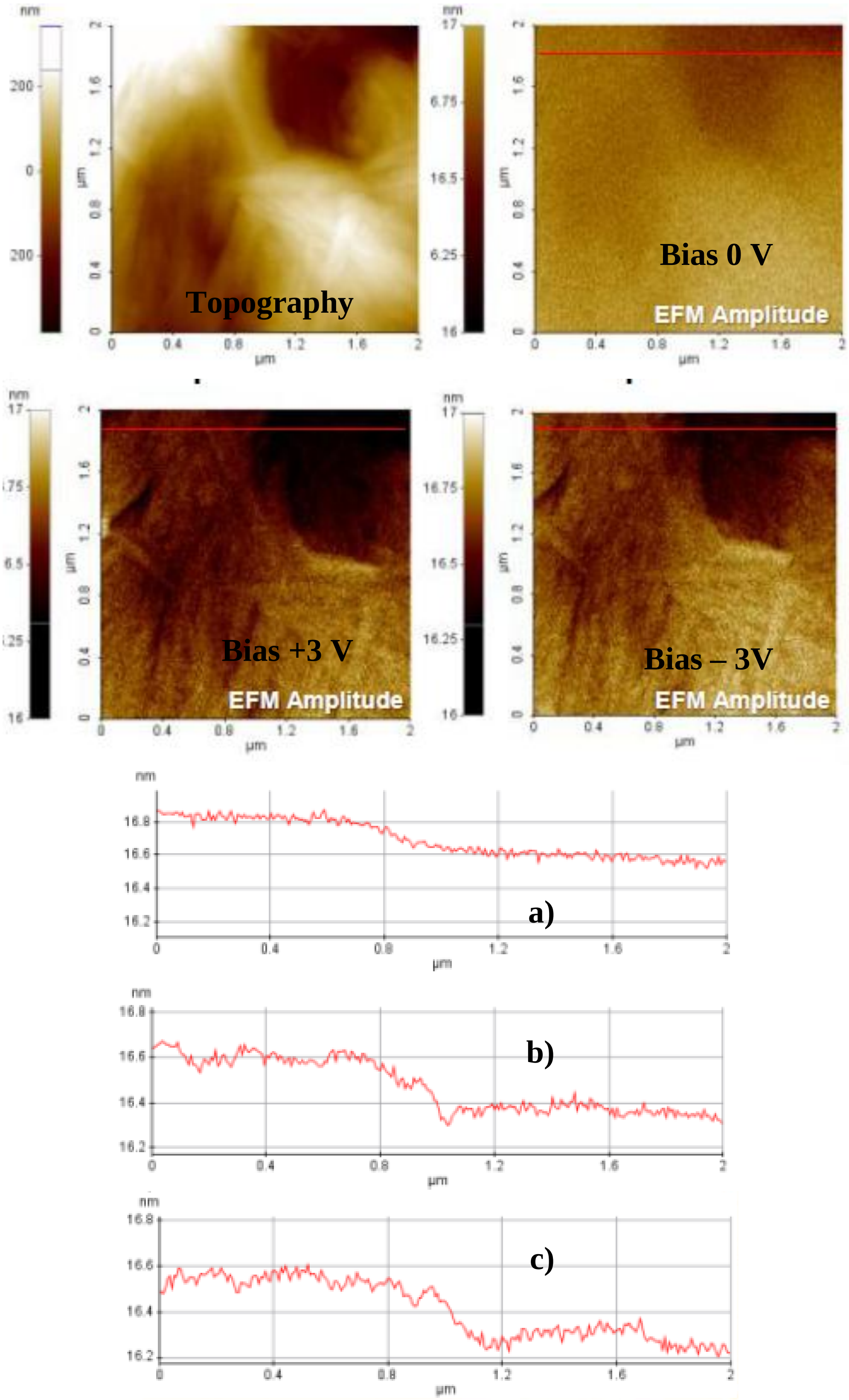

Figure 4.17 : Current signals of Cu^{+} exchanged samples measured with Internal EFM (a) 0 Bias, (b) +3V Bias, (c) -3V bias

5. CONCLUSIONS AND RECOMMENDATIONS

High-quality sepiolite nanofibers deliberated by high-speed mixers and separated from impurities using gravity separation techniques. After obtained the sepiolite fibrous, Ag^{+} and Cu^{2+} loaded sepiolites were prepared. According to adsorption isotherms, antibacterial activity of Ag^{+} and Cu^{2+} loaded sepiolite fibers was tested for *E.coli* and *S.aureus* by two common methods: serial dilution and disk diffusion method. Results showed that minimum inhibitory concentrations of each solutions were determined as 50mg/L Ag^{+} and 100mg/L Cu^{2+} - loaded sepiolite samples, respectively.

AFM study showed that sepiolite fibers have two dimensions in nanoscale. Also, the relation between topography and the electrical conductivity of the sepiolite samples were measured revealed with EFM and I-AFM measurements. External I-AFM mode referred to the I-AFM that uses the external low noise current amplifier named as Ultra-Low Noise Conductive AFM (ULCA), silver loaded sepiolite films showed promising results compared to the copper functionalized sepiolite films while raw sepiolite has no electrical conductivity. Each Ag^{+} ion functionalized sepiolite fibers show excellent antibacterial activity as well as good electrical conductivity. Both $Cu2^{+}$ and Ag^{+} ion loaded sepiolites were determined as antibacterial semiconductors. These activities will be increased with decreasing the surface roughness of the sepiolite inorganic films. Therefore, further experiments will be continued in the developing of new techniques to disperse the fibers more efficiently such as ultrasonic dispersion. It is obvious that these modified high-quality sepiolite nanofibers have big potential for nanotechnological and biomedical applications.

REFERENCES

Aguzzi, C., Cerezo P., Viseras C., Caramella C. (2007). Physical Modification of Nanofibers, *Appl. Clay Sci.*, *36*

Alvarez, E., Laffita, Y., Ruiz, E. (2012). High conducting sepiolite-graphenelike carbon nanocomposite from sugar residual as carbon source, Advances in Applied Ceramics, 111, 8, 508-511.

Ausman K. D., Piner R., Lourie O., Ruoff R. S., Korobov M. (2000). Organic solvent dispersions of single-walled carbon nanotubes: toward solutions of pristine nanotubs, *Journal of Physical Chemistry B, 104, 38*, 8911–8915.

Benli B., Hao D., Celik M. (2012). The anisotropic characteristics of natural fibrous sepiolite as revealed by contact angle, surface free energy, AFM and molecular dynamics simulation, *Colloids and Surfaces A: Physicochem. Eng. Aspects, 408*, 22–31.

Bystrzejewski M., Huczko A., Lange H., Gemming T., Büchner B. (2010). Dispersion and diameter separation of multi-wall carbon nanotubes in aqueous solutions, *Journal of Colloid and Interface Science, 345, 2*, 138–142.

Callow M. E., Dubois, P. (2008). Preparation and characterisation of silicone-based coatings filled with carbon nanotubes and natural sepiolite and their application as marine fouling-release coatings, *Biofouling*, *24,* 291-302.

Caoa W. C., Wang L. J., Xieb X. L. (2012). Thermal Stability and Fire Retardancy of Polypropylene/Sepiolite Composite, *Fire and Polymers VI: New Advances in Flame Retardant Chemistry and Science, Chapter 25,* 391–406.

Čík, G. (2001). Study of fungicidal and antibacterial effect of the Cu(II)-complexes of thiophene oligomers synthesized in ZSM-5 zeolite channels, *Chemosphere*, *44*, 313–319.

Cong C. (2010). Thermal Insulation Coatings Containing Sepiolite Mineral Fibers and their Performance, *Advanced Materials Research*, 178, 318.

Cubillo, A.E. (2006). Antibacterial activity of copper monodispersed nanoparticles into sepiolite, *J Mater Sci*, *41*, 5208–5212.

Ding P., Pacek A.W. (2008). De-agglomeration of goethite nano-particles using ultrasonic comminution device, *Powder Technol.*, *187*, 1–10.

Eerdenbrugh B.V., Van den Mooter G., Augustijns P. (2008). Top-down production of drug nanocrystals: nanosuspension stabilization, miniaturization and transformation into solid products, *Int. J. Pharm.*, *364*, 64–75.

Felten A., Bittencour C. , Pireaux J. J., Van Lier G., Charlier J. C. (2005). Radio-frequency plasma functionalization of carbon nanotubes surface O2, NH3, and CF4 treatments, *Journal of Applied Physics, 98, 7*.

Garza, R. M. (2000). Silver supported on natural Mexican zeolite as an antibacterial material, *Micropor. Mesopor. Mat., 39*, 431–444.

Gómez, R. (2008). Bactericides of coliform microorganisms from wastewater using silver-clinoptilolite rich tuffs, *Appl. Clay. Sci,. 40*, 45–53.

Gonzalez-Dominguez J. M., Martınez-Rubi Y., Diez-Pascual M. (2012). Reactive fillers based on SWCNTs functionalized with matrix-based moieties for the production of epoxy composites with superior and tunable properties, *Nanotechnology, 23, 28.*

Haggenmueller R., Rahatekar S. S., Fagan J. A. (2008). Comparison of the quality of aqueous dispersions of single wall carbon nanotubes using surfactants and biomolecules, *Langmuir, 24, 9*, 5070–5078.

Higashitan K., Yoshida K., Tanise N., Murata H. (1993). Dispersion of coagulated colloids by ultrasonication, *Colloids Surf. A, 81*, 167–175.

Hu, C.H., Xia, M.S. (2006). Adsorption and antibacterial effect of copper-exchanged montmorillonite on Escherichia coli K88, *Appl. Clay. Sci., 31*, 180–184.

Huang N. (2010). Synergistic flame retardant effects between sepiolite and magnesium hydroxide in ethylene-vinyl acetate (EVA)matrix, *Polymer Letters*, 4, 4, 227–233

Inkyo M., Tahara T., Iwaki T., Iskandar F., Okuyama K. (2006). Experimental investigation of nanoparticle dispersion by beads milling with centrifugal bead separation, *J. Colloid Interface Sci., 304*, 535–540.

Kohut A., Ranjan S., Voronov A., Peukert W., Tokarev V., Bednarska O. (2006). Design of a new invertible polymer coating on a solid surface and its effect on dispersion colloidal stability, *Langmuir, 22*, 6498–6506.

Kohut A., Voronov A., Peukert W. (2007). An effective way to stabilize colloidal particles dispersed in polar and nonpolar media, *Langmuir, 23*, 504–508.

Laoutid F., Persenaire O., Bonnaud L. (2013), Flame retardant polypropylene through the joint action of sepiolite and polyamide, *Polymer Degradation and Stability, 98, 10*, 1972–1980.

Lavskaya Y. V., Bulusheva L. G., Okotrub A. V., Yudanov N. F., Vyalikh D. V. (2009). Comparative study of fluorinated single- and few-wall carbon nanotubes by X-ray photoelectron and X-ray absorption spectroscopy, *Carbon, 47, 7*, 1629–1636.

Lee J. U., Huh J., Kim K. H., Park C., Jo W. H. (2007). Aqueous suspension of carbon nanotubes via non-covalent functionalization with oligothiophene-terminated poly(ethylene glycol),"*Carbon, 4, 5,* 1051–1057.

Magaňa, S.M. (2008). Antibacterial activity of montmorillonites modified with silver, *J. Mol. Catal. A.: Chem., 281*, 192–199.

Malachová, K. (2009). Activity of antibacterial compounds supported on montmorillonite, *Appl. Clay Sci., 43*, 364–368.

Malachová, K. (2011). Antibacterial and antifungal activities of silver, copper and zinc montmorillonites, *Appl. Clay Sci., 53 (4)*, 642–645.

Mathiazhagan A., Rani J. (2011). Nanotechnology-A New Prospective in Organic Coating, *International Journal of Chemical Engineering and Applications, 2 , 4.*

Muller F., Peukert W., Polke R., Stenger F. (2004). Dispersing nanoparticles in liquids, *Int. J. Miner. Process., 7,* S31–S41.

Nativ-Roth E., Shvartzman-Cohen R., Bounioux C. (2007). Physical adsorption of block copolymers to SWNT and MWNT: a nonwrapping mechanism, *Macromolecules, 40, 10,* 3676–3685.

Özdemir, A. (2004). The antibacterial effect of heavy metal and cetylpyridinium-exchanged montmorillonites, *Appl. Clay Sci., 48 (2010)*, 319–323.

Pang J., Xu G., Yuan S., Tan Y., He F. (2009). Dispersing carbon nanotubes in aqueous solutions by a silicon surfactant: experimental and molecular dynamics simulation study, *Colloids and Surfaces A, 350,* 101–108.

Paredes J. I., Burghard M. (2004). Dispersions of individual single-walled carbon nanotubes of high length, *Langmuir, 20, 12,* 5149–5152.

Peng H., Alemany L. B., Margrave J. L., Khabashesku V. N. (2003). Sidewall carboxylic acid functionalization of single-walled carbon nanotubes, *Journal of the American Chemical Society, 125, 49*, 15174–15182.

Petrik, S. (2011). Industrial Production Technology for Nanofibers, in Nanofibers – *Production, Properties and Functional Applications*, Chapter 1.

Peukert W., Schwarzer H.C., Stenger F. (2005). Control of aggregation in production and handling of nanoparticles, *Chem. Eng. Process., 44,* 245–252.

Rout, T. K., Jha, G., Singh, A. K. (2003). Development of conducting polyaniline coating: a novelapproach to superior corrosion resistance, *Surf. Coat. Technol., 167*, 16–20.

Sabba Y., Thomas E. L. (2004). High-concentration dispersion of single-wall carbon nanotubes, *Macromolecules, 37, 13*, 4815–4820.

Santos, M.F. (2011). Bactericidal properties of bentonite treated with Ag^+ and acid, *International Journal of Mineral Processing, 100*, 51–53.

Segura J., Cid C. , Llano J., José G. (1987). Sepiolite-supported urease, *British Polymer Journal, 19, 6,* 517–522.

Soylemez S., Kanik F.E., Tarkuc S., Udum Y.A., Toppare L.A. (2013). Sepiolite modified conducting polymer based biosensor *Colloids and Surfaces B: Biointerfaces*, 111, Pages 549–555.

Strobel R., Baiker A., Pratsinis S.E. (2006). Aerosol flame synthesis of catalysts, *Adv. Powder Technol., 17,* 457–480.

Sunga G., Parka J. (2013). Fluorosilica/sepiolite hybrids for hydrophobic coating, *The Second Japan-Korea Joint Symposium on Polymer Nanohybrid Materials*, 19, 9, 547-556.

Tadros F. (1993). Industrial applications of dispersions, *Adv. Colloid Interface Sci.,* 46 l–47.

Top, A., Ülkü, S. (2004). Silver, zinc, and copper exchange in a Na-clinoptilolite and resulting effect on antibacterial activity, *Appl. Clay Sci., 27*, 13–19.

Utegulov Z. N., Mast D. B., He P., Shi D., Gilland R. F. (2005). Functionalization of single-walled carbon nanotubes using isotropic plasma treatment: resonant Raman spectroscopy study, *Journal of Applied Physics, vol. 97, no. 10*, 1–4.

Wang Y., Iqbal Z., Malhotra S. V. (2005). Functionalization of carbon nanotubes with amines and enzymes, *Chemical Physics Letters, 402,* 96–101.

Wang Y., Iqbal Z., Mitra S. (2006). Rapidly functionalized, water-dispersed carbon nanotubes at high concentration, *Journal of the American Chemical Society, 128, 1*, 95–99.

Vaisman L., Marom G., Wagner H. D. (2006). Dispersions of surface-modified carbon nanotubes in water-soluble and water-insoluble polymers, *Advanced Functional Materials, 16, 3,* 357–3632006.

Xia, M.S. (2005). Effects of copper bearing montmorillonite on the growth performance, intestinal microflora and morphology of weanling pigs, *Anim. Feed Sci. Tech,. 118*, 307–317.

Xin X., Xu G., Zhao T. (2008). Dispersing carbon nanotubes in aqueous solutions by a starlike block copolymer, *Journal of Physical Chemistry C, 112, 42*, 16377–16384,.

Zhao, D. (2006). Preparation and characterization of Mingguang palygorskite supported with silver and copper for antibacterial behaviour, *Appl. Clay. Sci., 33*, 161–170.

Zhiping L., Fei Y. (2007). Synthesis and Properties of Polystyrene/sepiolite Composite, *Materials Engineering and Sciences Division Annual Meeting*, Salt Lake City.

Zhu J., Yudasaka M., Zhang M., Iijima S. (2004). Dispersing carbon nanotubes in water: a noncovalent and nonorganic way, *Journal of Physical Chemistry B, 108, 31*, 11317–11320.

Url – 1 <http://www.frufrus.ca/Ponds-Clear-Balance-Smooth-Pores-Pore Tightening-Facial-Foam-Glacial-Clay>, date retrieved 20.11.2013

Url – 2 <http://amieskincare.com/product/amie-spring-clean-cooling-clay mask>, date retrieved 20.11.2013

Url – 3 <http://bielendaprofessional.pl/en/products/antibacterial-mask-with green-clay>, date retrieved 20.11.2013

Url – 4 <http://www.biologie.uni-hamburg.de>, date retrieved 20.11.2013

CURRICULUM VITAE

Name Surname: Nihan Cansu YALIN

Place and Date of Birth: Istanbul, 1984

Address: Hızırbey Cad. 148/22 Kadıköy/Istanbul 34732

E-Mail: cansuyalin@gmail.com

B.Sc.: Istanbul University, Biology

Professional Experience and Rewards:

03.2012 – 03.2013 : Istanbul Technical University, Mineral Processing Department Researcher (ITU BAP Project – Developing Antimicrobial Sepiolite Clay NanoFibers)

07.2011 – 03.2012 : Istanbul Technical University, Mineral Processing Department Researcher (111M026 Tubitak Project – Using Sepiolite Clay NanoFibers in Sensor Technology)

PUBLICATIONS/PRESENTATIONS ON THE THESIS

Benli, B., Yalın, C., Electrical Characterization of Copper or Silver Functionalized Sepiolite Nanofiber Coatings by Current Atomic Force Microscopy (I-AFM), Nanoenergy, UK. 16-19 February 2014.

Yalın C., Benli B., "Antibacterial nanofiber production from fiber structure sepiolite", XV Balkan Mineral Processing Congress, Bulgaria, 12-16 June 2013.

Benli, B., Yalın, C., "Novel potential of nanoclay and nanoclay based electrodes", Electrochem 2011, England, 5-6 September 2011.

Yalın C., Özer M., Benli B., "Enhancement of fiber structured sepiolite clay by gravity separation", 11th World Filtration Congress, Austria, 16-20 April 2012.